

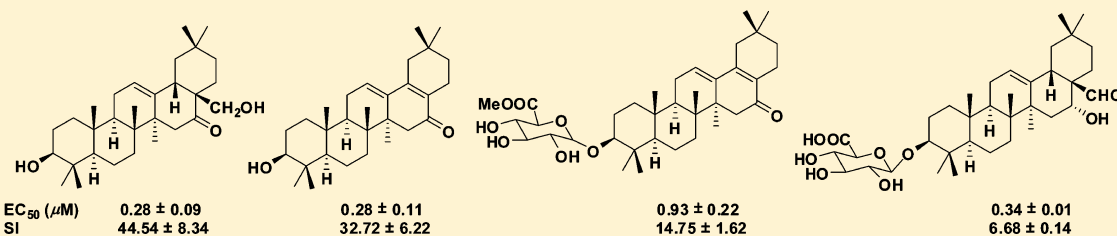
Oleanane Triterpenes from the Flowers of *Camellia japonica* Inhibit Porcine Epidemic Diarrhea Virus (PEDV) Replication

Jun-Li Yang,^{†,§} Thi-Kim-Quy Ha,^{†,§} Basanta Dhodary,[†] Euisun Pyo,[†] Ngoc Hieu Nguyen,[†] Hyoomoon Cho,[†] Eunhee Kim,[‡] and Won Keun Oh^{*,†}

[†]Korea Bioactive Natural Material Bank, Research Institute of Pharmaceutical Sciences, College of Pharmacy, Seoul National University, Sillim-dong, Gwanak-gu, Seoul 151-742, Republic of Korea

[‡]Choong Ang Vaccine Laboratory, 59-3 Hwaam-dong, Yuseong-gu, Daejeon 305-348, Republic of Korea

Supporting Information



ABSTRACT: Porcine epidemic diarrhea virus (PEDV) infections have resulted in a severe economic loss in the swine industry in many countries due to no effective treatment approach. Fifteen oleanane triterpenes (**1–15**), including nine new ones (**1–4** and **10–14**), were isolated from the flowers of *Camellia japonica*, and their molecular structures were determined by extensive spectroscopic methods. These compounds were evaluated for their antiviral activity against PEDV replication, and the structure–activity relationships (SARs) were discussed. Compounds **6**, **9**, **11**, and **13** showed most potent inhibitory effects on PEDV replication. They were found to inhibit PEDV genes encoding GP6 nucleocapsid, GP2 spike, and GP5 membrane protein synthesis based on RT-PCR data. Western blot analysis also demonstrated their inhibitory effects on PEDV GP6 nucleocapsid and GP2 spike protein synthesis during viral replication. The present study suggested the potential of compounds **6**, **9**, **11**, and **13** as promising scaffolds for treating PEDV infection via inhibiting viral replication.

INTRODUCTION

Coronaviruses (CoVs), first identified in the 1960s, are one type of enveloped viruses with positive strand RNA genome.¹ They contain the largest genome to date, ranging from approximately 26 to 32 kilobases.² During CoVs replication, genes encoding the viral structural proteins, including nucleocapsid (N), membrane (M), spike (S), and envelope (E), are key elements for viral integrity. CoVs infections are a major cause of enteric, respiratory, and central nervous system diseases in humans. Between November 2002 and July 2003, an outbreak of SARS-CoV infections in Hong Kong caused severe acute respiratory syndrome (SARS) of more than 8000 individuals and 774 fatalities worldwide.³ CoVs are also able to cause a range of seasonal or local epidemics of gastrointestinal and respiratory diseases in farm animals, which are fatal in young animals. There are four common CoVs infecting animals, including porcine epidemic diarrhea virus (PEDV), canine coronavirus (CCV), avian infectious bronchitis virus (IBV), and transmissible gastroenteritis coronavirus (TGEV).⁴

Porcine epidemic diarrhea virus (PEDV), an enveloped and single-stranded RNA virus from the genus *Alphacoronavirus* and family Coronaviridae, can spread via vertical transmission through lactation or the fecal-oral route.⁵ By targeting the epithelial cells of the small intestine, PEDV can cause severe

mucosal atrophy and malabsorption and result in acute and lethal diarrhea in piglets.⁶ PEDV infection can cause a high mortality in piglets and fattening swine, with almost 100% for one-week old piglets, and these diseases have resulted in a considerable economic loss in the swine industry in swine-producing countries.⁷ PEDV infection is becoming increasingly problematic over the world, including Europe, Asia, and America. Since 2010, PEDV infections have swept China, causing more than 1 million fatalities of newborn piglets.⁸ In the USA, with the first detection of PEDV in Ohio in 16 April of 2013, this lethal virus is spreading to 17 states with 40–50 new cases diagnosed each week, which could cause an epidemic with loss of millions of dollars.^{7,9} In concern about the control and eradication of PEDV infection, generous efforts have been made with major focus on preventive therapy by vaccination. Basically, live attenuated virus and the gene containing spike protein sequences are being tested as vaccines.¹⁰ P-SV, a commercial attenuated virus vaccine, has been developed in Japan. However, not all sows treated with P-SV developed stable lactation-induced immunity.¹¹ Another example is that DR13, an oral vaccine for preventing PEDV infections in South

Received: September 27, 2014

Published: January 8, 2015

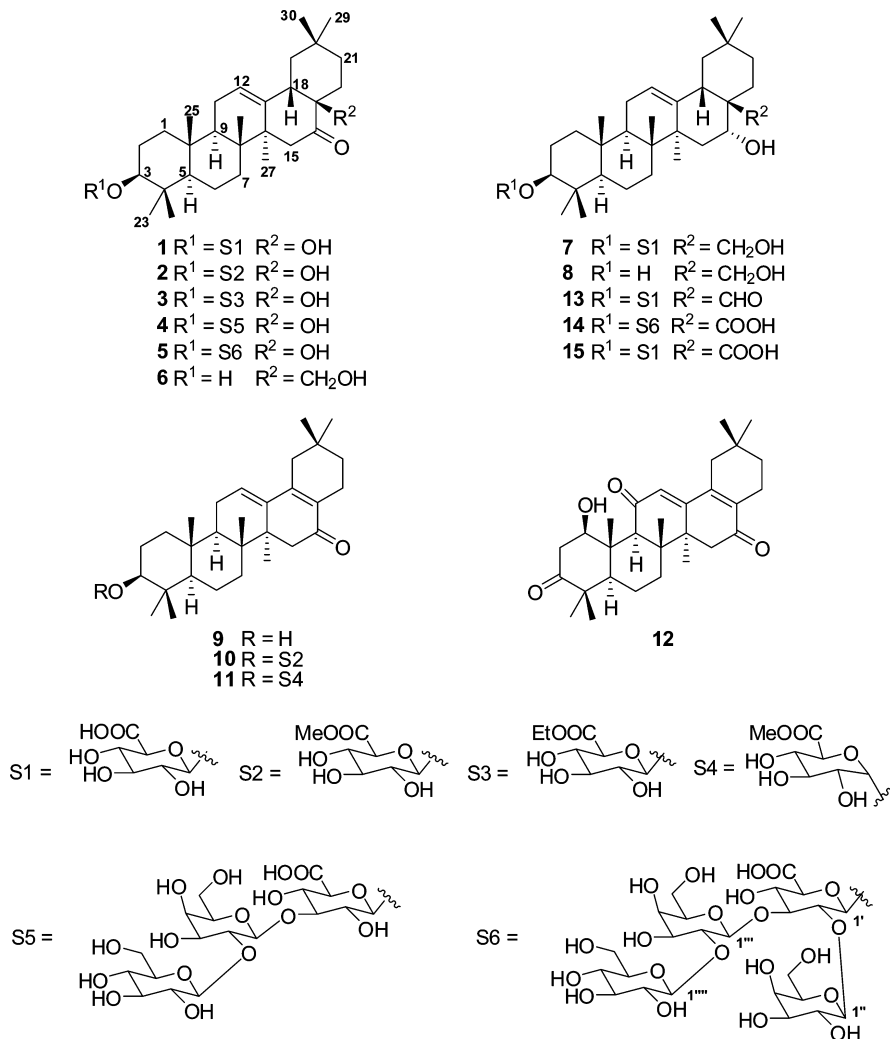


Figure 1. Oleanane triterpenes **1–15** isolated from the flowers of *Camellia japonica*.

Korea, is still not able to significantly alter the duration of virus shedding, indicating the immune protection in challenged piglets.¹² Thus a noble effective control strategy may be the benefit to prevent such infections.

There are three key steps throughout the virus life cycle: viral entry, viral replication, and viral assembly and budding. Among these, viral replication is the core of viral life cycle, and most current antiviral agents target this stage,¹³ which make it an exciting and promising target for antiviral research. Compounds inhibiting viral replications are virus-specific and chemically diverse. These properties match current effects to discover specific antiviral agents.¹⁰

Natural products have been regarded as a rich source of novel chemical entities with unique pharmacological activities. Of them, oleanane saponins have been reported to show phytotoxicity,^{14a} antileishmanial activity,^{14b,c} the inhibition on HCV entry,^{14d} and membrane permeabilizing effects,^{14e} as well as the hemolytic,^{14f} anti-inflammatory,^{14g} and HIV inhibitory activities.^{14g} Structure–activity relationship (SAR) studies on these bioactive saponins indicated that hydroxylation at C-3 positively influence the phytotoxicity,^{14a} while hydroxylation at C-16 would increase the antileishmanial activity,^{14b} the inhibition on HCV entry,^{14d} and the membrane permeabilizing effects.^{14e} Furthermore, the glycosylation at OH-3 and COOH-28 also contribute to the antileishmanial activity^{14b} and

inhibition on HCV entry,^{14d} respectively. However, coglycosylation at OH-3 and COOH-28 would be another approach for enhancing the potency of such compounds for membrane permeabilizing.^{14e}

We have screened thousands of plant extracts for antiviral activity against PEDV. During this process, it was found that a 70% ethanol extract of *Camellia japonica* flowers showed potential inhibitory effects on PEDV replication. *Camellia japonica* L. (Theaceae) is an evergreen tree widely distributed in Korea, China, and Japan.¹⁵ Flowers of *C. japonica*, known as Camellia flowers, have long been used as a traditional medicine for tonic, anti-inflammatory, and stomachic, as well as treating hematemesis and bleeding due to internal and external injury.¹⁶ Bioassay-guided fractionation of this active extract afforded nine previously undescribed oleanane triterpenes (**1–4** and **10–14**), as well as six previously reported but no antiviral studied oleanane triterpenes (**5–9** and **15**). Herein, the antiviral activities, including action of mechanisms, against PEDV of all isolates were evaluated and a brief structure–activity relationship was also discussed.

RESULTS AND DISCUSSION

Isolation and Structure Elucidation. The flowers of *C. japonica* were extracted with 70% EtOH using sonication. By means of diverse chromatographic methods, including silica gel,

Table 1. ^{13}C NMR Data for Compounds 1–3 and 10–13

no.	1 ^a	2 ^a	3 ^a	10 ^b	11 ^b	12 ^b	13 ^c
1	40.0, CH ₂	39.6, CH ₂	40.4, CH ₂	38.7, CH ₂	38.4, CH ₂	79.0, CH	38.5, CH ₂
2	27.4, CH ₂	27.2, CH ₂	27.8, CH ₂	27.1, CH ₂	28.3, CH ₂	43.5, CH ₂	27.1, CH ₂
3	91.3, CH	91.0, CH	91.8, CH	90.0, CH	84.1, CH	214.8, C	90.8, CH
4	40.5, C	40.2, C	41.0, C	40.4, C	40.6, C	43.9, C	42.7, C
5	57.3, CH	56.9, CH	57.7, CH	55.6, CH	55.7, CH	50.9, CH	57.0, CH
6	19.6, CH ₂	19.2, CH ₂	20.0, CH ₂	18.0, CH ₂	18.4, CH ₂	18.9, CH ₂	19.3, CH ₂
7	34.5, CH ₂	34.1, CH ₂	34.9, CH ₂	33.4, CH ₂	33.6, CH ₂	32.3, CH ₂	34.2, CH ₂
8	41.3, C	41.1, C	41.9, C	39.0, C	40.6, C	42.8, C	41.8, C
9	48.4, CH	48.0, CH	48.8, CH	46.1, CH	46.3, CH	61.2, CH	48.1, CH
10	38.2, C	37.9, C	38.6, C	36.6, C	38.4, C	42.7, C	37.8, C
11	24.4, CH ₂	23.9, CH ₂	24.7, CH ₂	24.1, CH ₂	24.3, CH ₂	202.3, C	24.5, CH ₂
12	125.7, CH	125.4, CH	126.2, CH	126.8, CH	126.7, CH	125.0, CH	124.5, CH
13	143.1, C	142.8, C	143.5, C	139.2, C	139.4, C	158.1, C	144.2, C
14	48.9, C	49.0, C	49.3, C	44.9, C	46.3, C	46.9, C	42.7, C
15	44.3, CH ₂	43.9, CH ₂	44.7, CH ₂	40.4, CH ₂	40.6, CH ₂	40.0, CH ₂	33.4, CH ₂
16	217.3, C	217.0, C	217.8, C	200.4, C	200.4, C	198.0, C	73.9, CH
17	77.9, C	77.6, C	77.5, C	129.0, C	129.3, C	138.6, C	52.2, C
18	53.8, CH	53.4, CH	54.2, CH	146.8, C	146.9, C	144.0, C	41.8, CH
19	48.4, CH ₂	48.6, CH ₂	48.8, CH ₂	44.9, CH ₂	46.4, CH ₂	46.2, CH ₂	47.4, CH ₂
20	32.0, C	31.6, C	32.4, C	29.2, C	29.4, C	29.1, C	31.3, C
21	38.3, CH ₂	37.9, CH ₂	38.7, CH ₂	34.3, CH ₂	34.5, CH ₂	33.7, CH ₂	33.4, CH ₂
22	32.0, CH ₂	31.6, CH ₂	32.4, CH ₂	20.6, CH ₂	20.8, CH ₂	21.4, CH ₂	27.2, CH ₂
23	27.7, CH ₃	28.5, CH ₃	28.2, CH ₃	28.2, CH ₃	28.3, CH ₃	28.3, CH ₃	28.5, CH ₃
24	17.4, CH ₃	17.0, CH ₃	16.8, CH ₃	16.7, CH ₃	16.8, CH ₃	19.9, CH ₃	17.0, CH ₃
25	16.1, CH ₃	15.9, CH ₃	15.9, CH ₃	15.8, CH ₃	15.4, CH ₃	12.9, CH ₃	16.1, CH ₃
26	18.4, CH ₃	18.0, CH ₃	18.4, CH ₃	18.0, CH ₃	18.3, CH ₃	19.5, CH ₃	17.9, CH ₃
27	27.3, CH ₃	27.3, CH ₃	28.1, CH ₃	23.0, CH ₃	23.2, CH ₃	21.9, CH ₃	27.2, CH ₃
28							207.0, CH
29	33.4, CH ₃	33.0, CH ₃	33.8, CH ₃	28.6, CH ₃	28.84, CH ₃	29.1, CH ₃	33.4, CH ₃
30	25.0, CH ₃	23.9, CH ₃	25.4, CH ₃	28.2, CH ₃	28.81, CH ₃	28.3, CH ₃	24.5, CH ₃
1'	107.3, CH	107.1, CH	107.9, CH	105.0, CH	95.1, CH		106.8, CH
2'	75.7, CH	75.3, CH	75.4, CH	75.5, CH	71.6, CH		75.4, CH
3'	78.1, CH	77.5, CH	78.3, CH	77.3, CH	74.2, CH		78.1, CH
4'	73.6, CH	73.3, CH	74.0, CH	73.7, CH	71.7, CH		73.9, CH
5'	77.8, CH	76.7, CH	76.1, CH	76.7, CH	71.1, CH		77.9, CH
6'	173.2, C	171.5, C	171.8, C	170.0, C	170.9, C		173.2, C
OMe		52.8, CH ₃		52.8, CH ₃	53.0, CH ₃		
OEt			63.2, CH ₂				
			20.0, CH ₃				

^aRecorded in methanol-d₄ and 125 MHz. ^bRecorded in CDCl₃ and 125 MHz. ^cRecorded in methanol-d₄ and 150 MHz.

RP-C₁₈, LH-20, and HPLC, nine new (**1–4** and **10–14**) and six known (**5–9** and **15**) oleanane triterpenes (Figure 1) were purified and obtained.

Compound **1** was obtained as a white powder with $[\alpha]_D^{25} -50.0$ (*c* 0.1, MeOH). Its molecular formula C₃₅H₅₄O₉ was deduced from HRFABMS of *m/z* 641.3648 [M + Na]⁺ (calcd 641.3666), indicating nine degrees of unsaturation. The IR spectrum showed absorptions for hydroxy (3381 cm⁻¹), carbonyl (1706 cm⁻¹), and olefin (1664 cm⁻¹) functionalities. Acid hydrolysis of **1** with 5% aqueous H₂SO₄–1,4-dioxane afforded D-glucuronic acid, based on gas chromatography analysis following treatment with L-cysteine methyl ester hydrochloride and TMS derivatization,¹⁷ and coupling pattern of the anomeric proton (*d*, *J* = 7.7 Hz) indicated a β configuration for the glucuronopyranosyl unit.¹⁸ Besides, the ¹H and ¹³C NMR spectroscopic data (Table 1) revealed one oxymethine signal (δ_H 3.17, 1H, dd, *J* = 11.6, 4.0 Hz; δ_C 91.3), a trisubstituted olefin system (δ_H 5.39, 1H, br t, *J* = 3.6 Hz; δ_C 143.1, 125.7), one oxygenated quaternary carbon (δ_C 77.9), and

one ketone carbon (δ_C 217.3), as well as seven tertiary methyls (δ_H 1.14, 1.10, 1.06, 0.99, 0.96, 0.86, 0.85). The above observations displayed signals characteristic of an oleanane triterpene glycoside. Further analysis on HSQC and HMBC experiments (Figure 2) indicated that compound **1** possessed the same aglycone part as camellioside A,¹⁹ which was connected with a β -D-glucuronopyranosyl moiety at C-3, proven by HMBC correlations as follows: from H-3 (δ_H 3.17, 1H, dd, *J* = 11.6, 4.0 Hz) to C-1' (δ_C 107.3), and H-1' (δ_H 4.37, 1H, d, *J* = 7.7 Hz) to C-3 (δ_C 91.3). The coupling pattern of H-3 (dd, *J* = 11.6, 4.0 Hz) suggested the α -orientation of this proton,¹⁶ which was proven by the ROESY correlation from H-3 (δ_H 3.17) to H-5 (δ_H 0.80). The chemical shifts of C-16, C-17, C-18, and C-22 of **1** (δ_{C-16} 214.7, δ_{C-17} 76.0, δ_{C-18} 52.3, δ_{C-22} 31.2, in pyridine-d₅), similar to those of camellioside A (δ_{C-16} 214.9, δ_{C-17} 76.3, δ_{C-18} 52.7, δ_{C-22} 31.5, in pyridine-d₅),¹⁹ were used to support the β -orientation of OH-17. Finally, compound **1** was determined as camellenodiol 3-O- β -D-glucuronopyranoside.

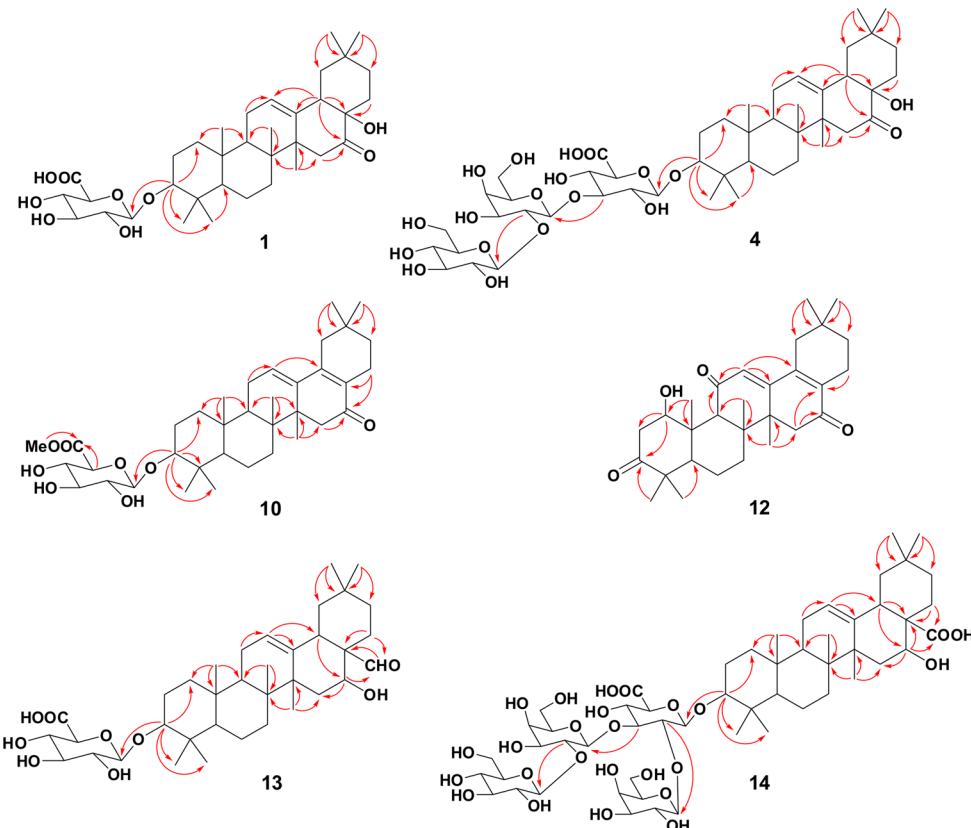


Figure 2. Key HMBC correlations (from H to C) for compounds **1**, **4**, **10**, and **12–14**.

The molecular formula of compound **2**, a white powder with $[\alpha]_D^{25} -31.7$ (*c* 0.1, MeOH), was analyzed for $C_{36}H_{56}O_9$ by HRFABMS (*m/z* 655.3820 [$M + Na$]⁺, calcd 655.3822). A β -D-glucuronopyranosyl unit was present in the structure of **2** based on GC analysis and coupling pattern of the acid hydrolysis product.^{17,18} Compound **2** demonstrated almost superimposable ¹H and ¹³C NMR data (Table 1) with those for **1**, and the major difference was the presence of one additional oxymethyl group (δ_H 3.76, 3H, s; δ_C 52.8) in **2**. An HMBC experiment revealed that this oxymethyl group showed a correlation to C-6' (δ_C 171.5), which suggested methyl esterification of the carboxylic group of the β -D-glucuronopyranosyl moiety. Consequently, compound **2** was elucidated as camellenodiol 3-O-6'-methoxy- β -D-glucuronopyranoside.

Compound **3**, compared with **2**, had closely similar NMR pattern and showed 14 more mass units by HRESIMS (*m/z* 669.3990 [$M + Na$]⁺, calcd 669.3979). Same as **1** and **2**, acid hydrolysis of **3** released D-glucuronic acid,¹⁷ and the coupling constant *J* = 7.8 Hz indicated a β configuration of this glucuronopyranosyl moiety.¹⁸ Analysis of the ¹H and ¹³C NMR data (Table 1) of **3** suggested the occurrence of one ethoxy group (δ_H 4.21, 2H, q, *J* = 6.8 Hz; 1.28, 3H, t, *J* = 6.8 Hz; δ_C 63.2, 20.0), which showed a HMBC correlation to C-6' (δ_C 171.8) of the β -D-glucuronopyranosyl unit. Thus, compound **3** was determined as camellenodiol 3-O-6'-ethoxy- β -D-glucuronopyranoside. Compound **3** was proven to be an artifact due to its absence in a later crude extract based on LC-MS and NMR analysis.

Compound **4**, with $[\alpha]_D^{25} -27.0$ (*c* 0.1, MeOH), was assigned a molecular formula of $C_{47}H_{74}O_{19}$ by HRFABMS (*m/z* 965.4744 [$M + Na$]⁺, calcd 965.4722). Its NMR data (Table 2) was closely similar to those of **1** except for the values of the

sugar part. Acid hydrolysis of **4** afforded D-glucuronic acid, D-galactose, and D-glucose.¹⁷ Coupling constants of anomeric protons indicated β configurations for the glucuronopyranosyl (*J* = 7.8 Hz), galactopyranosyl (*J* = 7.6 Hz), and glucopyranosyl (*J* = 7.6 Hz) units.¹⁸ On the basis of HSQC and HMBC experiments (Figure 2), together with comparing the NMR data with those of camelliosides E and F,^{16a} the linkage pattern of three sugar units was constructed as in Figure 1. Finally, compound **4** was determined as camellenodiol 3-O-[β -D-glucopyranosyl(1 \rightarrow 2)- β -D-galactopyranosyl(1 \rightarrow 3)]- β -D-glucuronopyranoside.

Compound **10**, a white powder with $[\alpha]_D^{25} -20.7$ (*c* 0.1, MeOH), was shown to have a molecular formula $C_{36}H_{54}O_8$ by HRFABMS (*m/z* 615.3899 [$M + H$]⁺, calcd 615.3897). The IR absorptions at 1731 cm^{-1} (C=O) and 1653 cm^{-1} (C=C) and UV peak at λ_{\max} 298 nm indicated the existence of an extended conjugated α,β -unsaturated ketone moiety,^{19,20} which was supported by characteristic ¹³C NMR resonances at δ_C 200.4, 146.8, 139.2, 129.0, and 126.8. This moiety was determined as 12,17-dien-16-one based on HMBC correlations as follows: from H-12 (δ_H 6.12) to C-9 (δ_C 46.1), C-13 (δ_C 139.2), C-14 (δ_C 44.9), and C-18 (δ_C 146.8), and from H-15 (δ_H 2.60, 2.14) to C-13 (δ_C 139.2), C-16 (δ_C 200.4), and C-17 (δ_C 129.0). Further analysis of the NMR data implied that compound **10** possessed the same aglycone part as that of camellioside C with the difference in sugar moiety.¹⁹ A β -D-glucuronopyranosyl unit was identified in **10**,^{17,18} and it was attached to C-3 based on HMBC correlations from H-3 (δ_H 3.18) to C-1' (δ_C 105.0) and H-1' (δ_H 4.39) to C-3 (δ_C 90.0). In addition, one oxymethyl group (δ_H 3.81; δ_C 52.8) showed HMBC correlation to C-6' (δ_C 170.0), implying methyl esterification of the carboxylic group of the β -D-glucuronopyranosyl unit. The α -orientation of

Table 2. ^{13}C NMR Data for Compounds 4^a and 14^b

no.	4	14	sugar carbons	4	14
1	38.3, CH ₂	37.9, CH ₂	3-O- β -D-glucuronopyranosyl		
2	26.4, CH ₂	27.0, CH ₂	1'	105.6, CH	106.1, CH
3	90.7, CH	91.7, CH	2'	73.5, CH	79.6, CH
4	39.4, C	40.8, C	3'	84.7, CH	82.5, CH
5	55.6, CH	57.2, CH	4'	70.4, CH	71.9, CH
6	18.3, CH ₂	18.1, CH ₂	5'	77.3, CH	76.7, CH
7	33.2, CH ₂	33.1, CH ₂	6'	172.1, C	176.3, C
8	40.1, C	40.7, C	2'-O- β -D-galactopyranosyl		
9	46.9, CH	48.1, CH	1''		103.1, CH
10	36.8, C	37.1, C	2''		73.8, CH
11	23.8, CH ₂	25.0, CH ₂	3''		75.0, CH
12	124.0, CH	123.7, CH	4''		70.8, CH
13	142.6, C	145.4, C	5''		76.8, CH
14	48.1, C	42.4, C	6''		62.3, CH ₂
15	43.3, CH ₂	36.1, CH ₂	3''-O- β -D-galactopyranosyl		
16	215.2, C	75.1, CH	1'''	104.3, CH	101.5, CH
17	76.3, C	49.8, C	2'''	89.4, CH	82.9, CH
18	52.7, CH	42.5, CH	3'''	74.9, CH	75.8, CH
19	48.2, CH ₂	47.0, CH ₂	4'''	69.1, CH	70.8, CH
20	30.9, C	30.5, C	5'''	76.4, CH	77.0, CH
21	37.2, CH ₂	35.1, CH ₂	6'''	61.9, CH ₂	62.6, CH ₂
22	31.6, CH ₂	33.4, CH ₂	2'''-O- β -D-glucopyranosyl		
23	28.0, CH ₃	28.5, CH ₃	1''''	107.4, CH	106.2, CH
24	16.7, CH ₃	17.0, CH ₃	2''''	76.3, CH	76.7, CH
25	15.3, CH ₃	16.0, CH ₃	3''''	79.0, CH	78.1, CH
26	17.6, CH ₃	18.0, CH ₃	4''''	71.5, CH	71.9, CH
27	27.1, CH ₃	27.2, CH ₃	5''''	79.0, CH	78.4, CH
28		180.6, C	6''''	64.4, CH ₂	62.8, CH ₂
29	32.7, CH ₃	33.1, CH ₃			
30	23.6, CH ₃	25.0, CH ₃			

^a Recorded in pyridine-*d*₅ and 125 MHz. ^b Recorded in methanol-*d*₄ and 150 MHz.

H-3 was determined based on its coupling pattern (dd, $J = 11.5, 4.3$ Hz)¹⁶ and ROESY correlation between H-3 ($\delta_{\text{H}} 3.18$) and H-5 ($\delta_{\text{H}} 0.79$). Finally, compound **10** was determined as 3 β -hydroxy-28-norolean-12,17-dien-16-one 3-*O*-6'-methoxy- β -D-glucuronopyranoside.

Compound **11** showed the same molecular formula C₃₆H₅₄O₈ as that of **10** by HRFABMS (*m/z* 615.3884 [M + H]⁺, calcd 615.3897). The IR, UV, and NMR spectra exhibited that **11** possessed the same aglycone part as that of **10**, which was confirmed by HSQC and HMBC experiments, with the clear different signals ascribed to sugar units. Acid hydrolysis of **11** released D-glucuronic acid, and the coupling constant of anomeric proton ($J = 4.0$ Hz) suggested a α configuration for this D-glucuronopyranosyl unit.¹⁸ In addition, a carboxylic acid methyl ester occurred at C-6' based on a HMBC correlation from an oxymethyl group ($\delta_{\text{H}} 3.82$) to C-6' ($\delta_{\text{C}} 170.9$). Consequently, compound **11** was elucidated as 3 β -hydroxy-28-norolean-12,17-dien-16-one 3-*O*-6'-methoxy- α -D-glucuronopyranoside.

Compound **12** was isolated as a white powder with $[\alpha]_{\text{D}}^{25} -10.0$ (*c* 0.1, MeOH) and was assigned a molecular formula C₂₉H₄₀O₄ by HRFABMS (*m/z* 453.3035 [M + H]⁺, calcd 453.3005). Its IR absorptions at 1643, 1645, and 1702 cm⁻¹ and UV peak at λ_{max} 311 nm, together with NMR data analysis (Table 1), suggested the existence of a 12,17-dien-16-one moiety,^{19,20} which was confirmed by HMBC experiments (Figure 2): from H-12 ($\delta_{\text{H}} 6.19$) to C-9 ($\delta_{\text{C}} 61.2$), C-13 ($\delta_{\text{C}} 158.1$), C-14 ($\delta_{\text{C}} 46.9$), and C-17 ($\delta_{\text{C}} 138.6$), and from H₂-15

($\delta_{\text{H}} 2.68, 2.37$) to C-13 ($\delta_{\text{C}} 158.1$), C-16 ($\delta_{\text{C}} 198.0$), C-17 ($\delta_{\text{C}} 138.6$), and C-18 ($\delta_{\text{C}} 144.0$). However, difference in the chemical shift and coupling pattern of H-12 between **12** ($\delta_{\text{H}} 6.19$, s) and **11** ($\delta_{\text{H}} 6.10$, br s) indicated that compound **12** possessed one more ketone group at C-11 ($\delta_{\text{C}} 202.3$). This proposal was supported by HMBC correlations from H-9 ($\delta_{\text{H}} 2.66$) and H-12 ($\delta_{\text{H}} 6.19$) to C-11 ($\delta_{\text{C}} 202.3$). Further analysis of HMBC spectrum revealed three important correlations from H-5 ($\delta_{\text{H}} 1.43$), H₃-23 ($\delta_{\text{H}} 1.09$), and H₃-24 ($\delta_{\text{H}} 1.07$) to a carbon at $\delta_{\text{C}} 214.8$, which indicated a ketone group attached at C-3. Moreover, an oxymethine proton at $\delta_{\text{H}} 3.90$ (dd, $J = 7.9, 2.8$ Hz) showing HMBC correlations to C-2 ($\delta_{\text{C}} 43.5$), C-3 ($\delta_{\text{C}} 214.8$), C-10 ($\delta_{\text{C}} 42.7$), and C-25 ($\delta_{\text{C}} 12.9$), together with the established molecular formula, supported the occurrence of an OH-1 group. The coupling pattern of H-1 (dd, $J = 8.0, 2.8$ Hz), which was similar to that of the known compound glochidionol (H-1: dd, $J = 8.1, 3.4$ Hz), was used to determine the β -orientation of OH-1.²¹ Therefore, compound **12** was established as 1 β -hydroxy-28-norolean-12,17-dien-3,11,16-trione.

Compound **13**, a white powder with $[\alpha]_{\text{D}}^{25} -46.4$ (*c* 0.1, MeOH), exhibited a molecular formula of C₃₆H₅₆O₉ on the basis of HRESIMS (*m/z* 655.3810 [M + Na]⁺, calcd 655.3822). Its IR peaks were characteristic for hydroxy (3410 cm⁻¹), olefin (1657 cm⁻¹), and carbonyl (1702 cm⁻¹) functionalities. Detailed analysis of ¹H and ¹³C NMR data demonstrated that compound **13** possessed the same aglycone part with that of camellioside F¹⁶ which was proven by HSQC and HMBC

experiments (Figure 2). The major difference was that there was only one sugar unit in **13**. After acid hydrolysis, D-glucuronic acid was released,¹⁷ and a β configuration was determined based on the coupling constant of anomeric proton ($J = 7.8$ Hz).¹⁸ This β -D-glucuronopyranosyl unit was attached at C-3, analyzed by HMBC correlations from H-3 (δ_H 3.18, dd, $J = 10.6, 3.9$ Hz) to C-1' (δ_C 106.8) and H-1' (δ_H 4.36, d, $J = 7.8$ Hz) to C-3 (δ_C 90.8). The coupling pattern of H-3 (dd, $J = 10.6, 3.9$ Hz) and H-16 (br s), which were similar to those of camellioside D (H-3, dd, $J = 11.9, 4.3$ Hz; H-16, br s),¹⁹ were used to identify the α -orientation of H-3 and β -orientation of H-16, respectively. Similarity of chemical shifts of C-16, C-17, C-18, and C-22 of compound **13** (δ_C : 73.1, 52.0, 41.3, and 27.5, respectively, in pyridine-d₅) and camellioside F (δ_C : 73.1, 51.4, 40.9, and 27.3, respectively, in pyridine-d₅)^{16a} indicated the β -orientation of the formyl group at C-17. These conclusions were further confirmed by ROESY correlations from H-3 (δ_H 3.18) and H-5 (δ_H 0.77), and from H-18 (δ_H 2.66) to H-16 (δ_H 4.27) and H-28 (δ_H 9.21). So, compound **13** was determined as 3 β ,16 α -dihydroxyolean-12-en-28-al 3-O- β -D-glucuronopyranoside.

The molecular formula of compound **14**, a white powder with $[\alpha]_D^{25} -18.3$ (*c* 0.1, MeOH), was determined as C₅₄H₈₆O₂₅ based on HRFABMS (*m/z* 1157.5317 [M + Na]⁺, calcd 1157.5356). Compound **14** exhibited very similar ¹H and ¹³C NMR data to those of camellioside F,^{16a} with the replacement of a formyl carbon (δ_C 205.8 in pyridine-d₅) in camellioside F by a carboxyl carbon (δ_C 180.6 in methanol-d₄) in **14**. This observation suggested that compound **14** had a carboxylic group at C-17, which was confirmed by HMBC correlations from H-16 (δ_H 3.79), H-18 (δ_H 2.19), and H₂-22 (δ_H 2.02, 1.57) to this carboxyl carbon at δ_C 180.6. Acid hydrolysis of **14** released D-glucuronic acid, D-glucose, and D-galactose,¹⁷ and β configurations were determined for the three sugar units based on the coupling patterns of anomeric protons ($J = 7.8$ Hz). The α -orientation of H-3 was determined by its coupling pattern (dd, $J = 11.0, 3.6$ Hz)¹⁹ and ROESY correlation from H-3 (δ_H 3.19) and H-5 (δ_H 0.78). The H-16 was analyzed as β -orientation on the basis of its coupling pattern (br s)¹⁹ and ROESY correlation from H-16 (δ_H 3.79) and H-18 (δ_H 2.19). The chemical shifts of C-16, C-17, C-18, and C-22 (δ_C : 74.9, 49.5, 42.3, and 33.5, respectively, in pyridine-d₅), which were closely similar to those of codonoposide (δ_C : 74.2, 50.0, 41.7, and 33.7, respectively, in pyridine-d₅),^{17c} were used to determine the β -orientation of the carboxylic group at C-17. Therefore, compound **14** was assigned as echinocystic acid 3-O-[β -D-galactopyranosyl(1 \rightarrow 2)]-[β -D-glucopyranosyl(1 \rightarrow 2)- β -D-galactopyranosyl(1 \rightarrow 3)]- β -D-glucuronopyranoside.

On the basis of spectroscopic and optical rotation data as well as literature values, other compounds were determined as camelliosides A (**5**),¹⁹ schimperinone (**6**),²² primulagenin A (**8**),²² 3 β -hydroxy-28-norleana-12,17-dien-16-one (**9**),²³ and echinocystic acid 3-O- β -D-glucuronopyranoside (**15**).²³ In addition, compound **7** was discovered from nature for the first time in the present study, which was obtained previously by a chemical reaction.²⁴

Inhibitory Effects of Camellia Triterpenes on PEDV Replication Analyzed by CPE Assay. The purified 15 oleanane-type triterpenes (**1–15**) were evaluated for their inhibitory effects on PEDV replication with azauridin as positive control. Vero cells were incubated with test compounds at different concentrations after inoculation with PEDV for 2 h. As shown in Table 3, compounds **6–9**, **11**, and

Table 3. Inhibition on PEDV Replication by Oleanane Triterpenes **1–15**

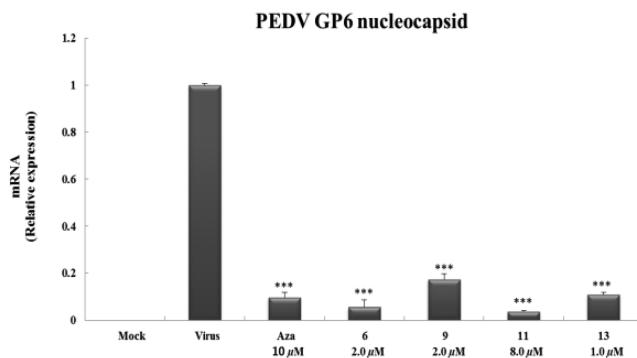
compd	CC ₅₀ (μ M)	EC ₅₀ (μ M)	SI
1	4.95 \pm 1.15	NA	
2	26.02 \pm 3.61	1.94 \pm 0.39	13.39 \pm 0.67
3	6.29 \pm 2.23	1.09 \pm 0.22	5.75 \pm 0.75
4	>20	NA	
5	5.91	NA	
6	12.47 \pm 0.97	0.28 \pm 0.09	44.54 \pm 8.34
7	7.23 \pm 0.87	0.91 \pm 0.07	7.99 \pm 0.28
8	0.81 \pm 0.07	0.06 \pm 0.02	12.98 \pm 2.34
9	9.32 \pm 1.19	0.28 \pm 0.11	32.72 \pm 6.22
10	27.29 \pm 5.63	2.90 \pm 0.25	9.40 \pm 1.04
11	13.72 \pm 1.35	0.93 \pm 0.22	14.75 \pm 1.62
12	13.95	NA	
13	2.25 \pm 0.11	0.34 \pm 0.01	6.68 \pm 0.14
14	>20	NA	
15	23.73 \pm 1.80	3.70 \pm 0.68	6.42 \pm 0.58
azauridin	48.17 \pm 5.15	3.37 \pm 0.71	14.30 \pm 1.24

13 exhibited potent inhibitory effects on PEDV replication, with EC₅₀ values at submicromolar range (0.06 \pm 0.02 to 0.93 \pm 0.22 μ M), which was stronger than that of positive control (EC₅₀ 3.37 \pm 0.71 μ M). In addition, compounds **6**, **9**, and **11** gave higher selective index (SI) values in this assay (44.54 \pm 8.34, 32.72 \pm 6.22, and 14.75 \pm 1.62, respectively), compared to azauridin (14.30 \pm 1.24), while compounds **7** and **13** showed lower SI values (7.99 \pm 0.28 and 6.68 \pm 0.14, respectively). Even though compound **8** gave considerable SI value (12.98 \pm 2.34), it demonstrated strong cytotoxicity (0.81 \pm 0.07 μ M) in this assay. Compounds **2**, **3**, **10**, and **15** also showed promising EC₅₀ values at low micromolar range (1.09 \pm 0.22 to 3.70 \pm 0.68 μ M). However, there were no obvious antiviral activity observed for compounds **1**, **4**, **5**, **12**, and **14** in this assay. Moreover, the inhibition on viral replication of compound **9** was further supported by a time-course study, the infectivity of PEDV particles assay, and cell protection assay for PEDV infection (Supporting Information).

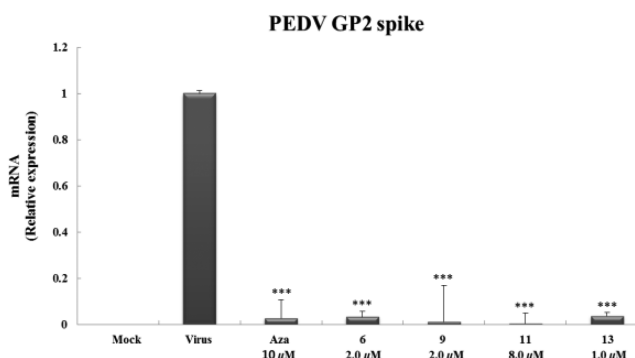
Structure–Activity Relationships (SARs) of Camellia Triterpenes on PEDV Replication Based on CPE Assay.

To discuss the SARs of Camellia triterpenes, the oleanane triterpenes (**1–15**) obtained in this investigation were divided into four groups based on the substitution pattern at the C-17 position: (1) substituted by OH (**1–5**), (2) substituted by CH₂OH (**6–8**), (3) occurrence of an olefinic double bond between C-17 and C-18 (**9–12**), (4) substituted by CHO or COOH (**13–15**). Biological data of group 1 (**1–5**) (Table 3) indicated that the monoglycosylation by glucuronopyranosyl moiety with esterification at C-6' could improve the antiviral property (comparing **2** and **3** with **1**, **4**, and **5**). Group 2 (**6–8**) demonstrated promising EC₅₀ values in the CPE assay (Table 3). In this group, the replacement of a hydroxy group by a ketone group at C-16 (comparing **6** with **8**) or monoglycosylation at C-3 (comparing **7** with **8**) induced lower cytotoxicity while keeping considerable antiviral effects. The antiviral profile of group 3 (**9–12**) (Table 3) indicated that monoglycosylation at C-3 could reduce cytotoxicity with keeping considerable antiviral activity (comparing **9** with **10** and **11**), and this trend depends on the type of attached sugar moieties. However, on the basis of the activity data of compounds **2** and **10** and compounds **6** and **9**, the existence of an olefinic double bond between C-17 and C-18 slightly decreased the SI value. From

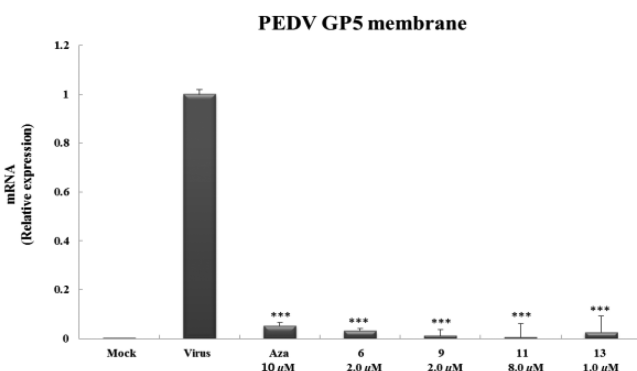
(A)



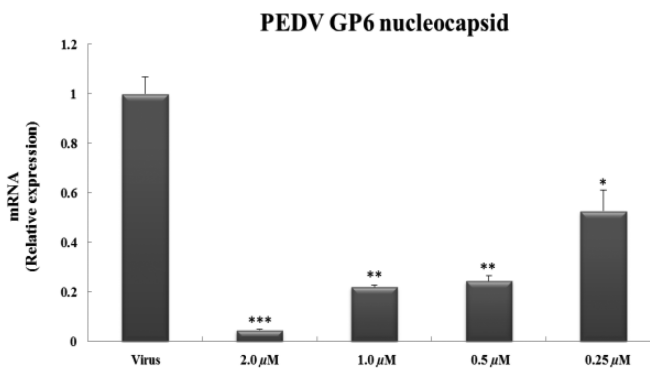
(B)



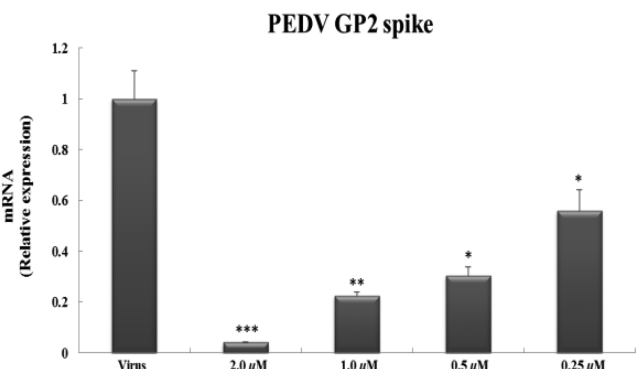
(C)



(D)



(E)



(F)

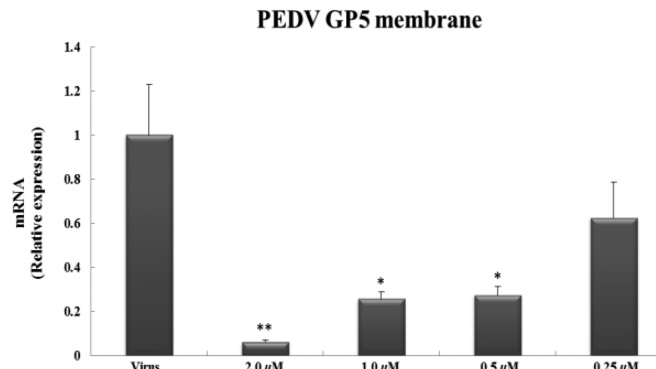


Figure 3. Inhibitory effects of camellia triterpenes on PEDV RNA expression encoding GP6 nucleocapsid, GP2 spike, and GP5 membrane protein, analyzed by RT-PCR. (A–C) Triterpenes 6, 9, 11, and 13 significantly inhibited PEDV RNA expression at concentrations of 2, 2, 8, and 1 μ M, respectively. (D–F) Compound 9 inhibited RNA expression in a dose-dependent manner.

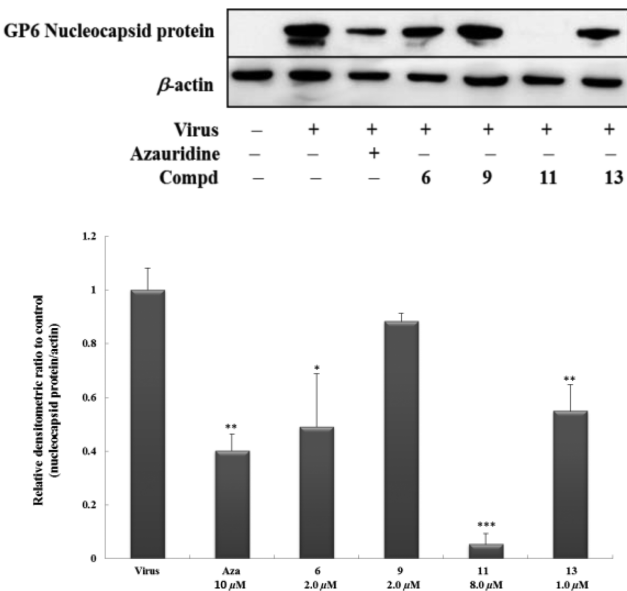
the antiviral effects of compounds 13–15 (Table 3), the substitution of a formyl group at C-17 increased anti-PEDV inhibition and also increased the cytotoxicity (comparing 13 with 15). However, multiple glycosylation at C-3 would significantly decrease the antiviral activity (comparing 14 with 15), and this observation was also supported by the data of compounds 4 and 5. In addition, on the basis of the results of compounds 7 and 15 (Table 3), the replacement of a carboxylic group by a hydroxymethyl group at C-17 improved the antiviral property. Through chemical diversity of Camellia triterpenes, the above observations allowed the outline of SARs for this compound class: (1) the coexistence of a ketone group at C-16 and a hydroxymethyl group at C-17 positively contribute to the anti-PEDV property of Camellia triterpenes, which is supported

by the comparison of biological data of compounds 6, 8, and 9, as well as the highest SI value of compound 6, (2) the multiple glycosylation at C-3 significantly decrease the anti-PEDV property of Camellia oleanane saponins, which is supported by the biological data of compounds 4, 5, and 14.

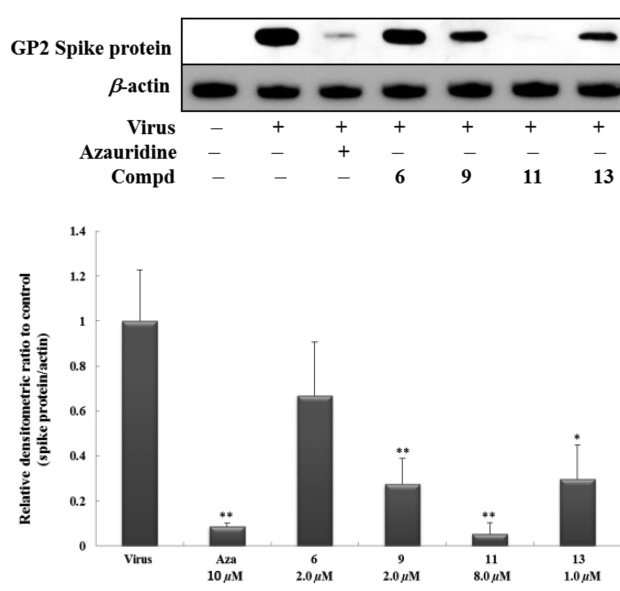
Inhibitory Effects of Camellia Triterpenes on Key Gene and Protein Synthesis during PEDV Replication.

During the PEDV life cycle, three key structural proteins, including spike, membrane, and nucleocapsid proteins, play a pivotal role.²⁵ The spike protein functions as a key regulator in viral entry step.²⁶ The membrane protein mainly regulates the viral assembly process,²⁷ and the nucleocapsid protein, which binds to viral RNA, is a basic protein associated with the

(A)



(B)



(C)

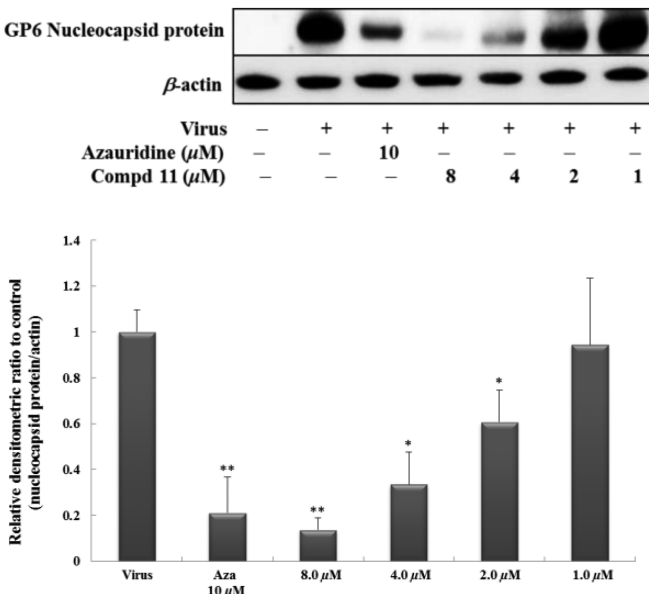


Figure 4. Inhibitory effects of camellia triterpenes on PEDV GP6 nucleocapsid and GP2 spike protein synthesis, using Western blot analysis. (A,B) Triterpenes **6**, **9**, **11**, and **13** inhibited PEDV nucleocapsid and spike protein synthesis at concentrations of 2, 2, 8, and 1 μ M, respectively. (C) Compound **11** inhibited the PEDV nucleocapsid protein synthesis in a dose-dependent manner.

genome.²⁸ Their biological functions place the three proteins as potential and promising targets for anti-PEDV research.

Considering CC₅₀, EC₅₀, and SI values as analyzed in CPE assay (Table 3), four structurally representative oleanane-triterpenes **6**, **9**, **11**, and **13** were selected and evaluated for their biological effects on several key genes and proteins required for PEDV replication. First, we measured the levels of intracellular viral RNA, encoding PEDV nucleocapsid, spike, and membrane protein synthesis. Vero cells, which were infected with PEDV, were treated with test compounds at different concentrations, at which compounds showed the strongest antiviral property. After 24 h, total RNA was isolated from cells and analyzed by real-time PCR, which was performed using selective primers for PEDV (Supporting Information). As

shown in Figure 3A–C, compounds **6**, **9**, **11**, and **13** were found to significantly reduce the RNA levels, associated with GP6 nucleocapsid, GP2 spike, and GP5 membrane protein, at concentrations of 2, 2, 8, and 1 μ M, respectively. All of them (**6**, **9**, **11**, and **13**) demonstrated comparable or stronger inhibitory effects on RNA expression, compared with azauridin that was used as positive control in this assay. The inhibitory effects of compounds **6**, **9**, **11**, and **13** on RNA expression were further evaluated at the same concentration of 0.25 μ M (Supporting Information). Furthermore, compound **9** was measured in detail, and it was found to inhibit PEDV RNA expression, encoding nucleocapsid, spike, and membrane protein, in a dose-dependent manner at concentrations of 2.0, 1.0, 0.5, and 0.25 μ M (Figure 3D–F). In addition, compounds **1**, **4**, and **5**

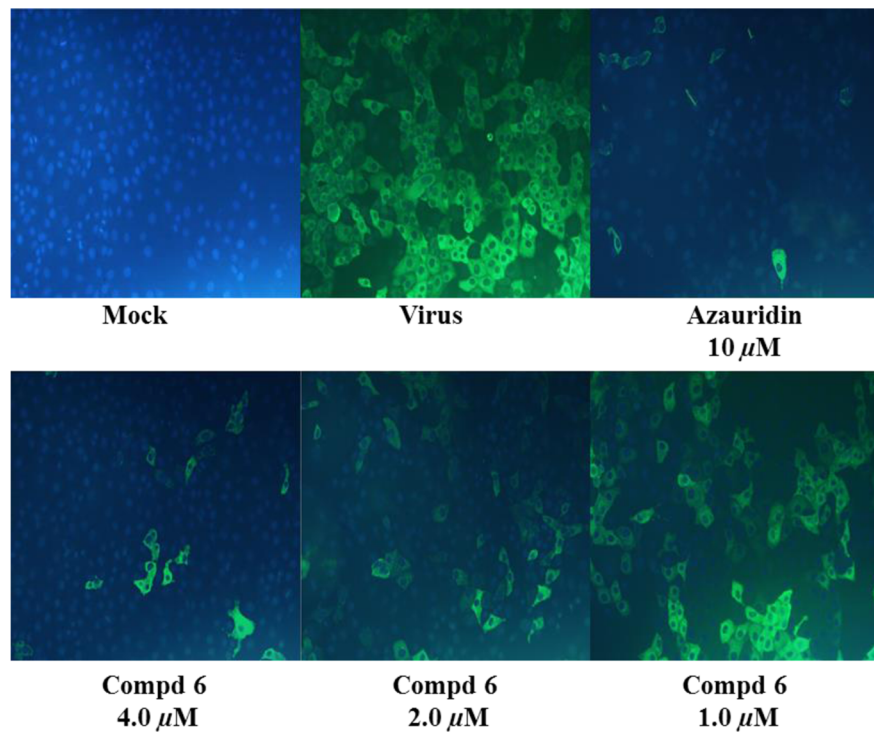


Figure 5. Immunofluorescence assay showed that compound **6** inhibited PEDV replication in a dose-dependent manner.

having no activity on PEDV RNA expression encoding GP6 nucleocapsid protein synthesis were further confirmed by RT-PCR analysis (Supporting Information).

On the basis of the above observations, compounds **6**, **9**, **11**, and **13** were further evaluated for their inhibitory effects on GP6 nucleocapsid and GP2 spike protein synthesis during PEDV replication. On the basis of Western blot analysis (Figure 4A,B), compound **11** showed significant inhibitory effects on PEDV nucleocapsid and spike protein synthesis, which was even stronger than that of azauridin. Compound **13** demonstrated considerable inhibitory effects, at the corresponding concentration to that in RT-PCR analysis. Moreover, compound **11** was found to inhibit nucleocapsid protein synthesis in a dose-dependent manner at concentrations of 8.0, 4.0, 2.0, and 1.0 μ M (Figure 4C).

On the basis of promising EC₅₀, SI value, and the potent inhibition on PEDV RNA expression, compound **6** was further evaluated for its inhibition on PEDV replication, analyzed by an immunofluorescence assay. As shown in Figure 5, virus-infected cells showed green fluorescence but not in mock-treated cells. The result implied that compound **6** showed marked inhibition on PEDV replication in a dose-dependent manner at concentrations of 4.0, 2.0, and 1.0 μ M. It was found that compound **6** showed a comparable effect at a concentration of 4 μ M, compared with azauridin at 10 μ M.

■ CONCLUSION

An acetone extract of the pericarp and leaves of *C. japonica* has been reported to show inhibitory effects on HIV type 1 protease.²⁹ In the present study, bioassay-guided fractionation of a 70% ethanol extract of *C. japonica* flowers yielded 15 oleanane triterpenes (**1–15**). A CPE assay, RT-PCR analysis, Western blot analysis, and immunofluorescence assay indicated that four representative triterpenes **6**, **9**, **11**, and **13** showed potent and promising inhibitory effects on PEDV replication by

targeting key structural protein synthesis and relevant gene expression. This study provided a new class of natural scaffolds that may be able to be developed as potential anti-PEDV agents via inhibiting viral replication. The clear SARs outlined will facilitate the further structure optimization of this compound class for developing novel antiviral agents. Furthermore, human corona viruses, like SARS, from the same Coronaviridae family, shares some similar replication mechanism with PEDV, and the development of SARS vaccine and PEDV vaccine shared similar theory.³⁰ Therefore, the anti-PEDV molecules obtained in this study could also be the noteworthy candidates for further investigation against the fatal human coronaviruses, including SARS.

■ EXPERIMENTAL SECTION

General Experimental Procedures. Optical rotations were analyzed by a JASCO P-2000 polarimeter (JASCO International Co. Ltd., Tokyo, Japan). UV data were determined using an Optizen 3220 UV spectrophotometer (Mekasys Co. Ltd., Daejon, Korea). IR spectra were recorded on a Nicolet 6700 FT-IR (Thermo Electron Corp., Waltham, MA, USA). NMR spectra were checked by Varian Unity Inova 500 and 600 MHz spectrometers at the College of Pharmacy, Seoul National University, Korea. HRFABMS and HRESIMS were recorded on a JEOL JMS 700 (JEOL, Ltd., Tokyo, Japan) and Agilent 6530 Q-TOF (Agilent Technologies, Inc., Santa Clara, CA, USA) spectrometer, respectively. Column chromatography (CC) was performed with silica gel (63–200 μ m particle size) and RP-C₁₈ (40–63 μ m particle size) obtained from Merck (Darmstadt, Germany), as well as Sephadex LH-20 (Sigma-Aldrich Corp., St. Louis, Missouri, USA). TLC profiles were checked on RP-C₁₈ F₂₅₄ and silica gel 60 F₂₅₄ plates. HPLC was performed on a Gilson System with an Optima Pak C₁₈ column (10 μ m particle size, 10 mm \times 250 mm; RS Tech, Seoul, Korea) and a UV detector. All solvents used for extraction and isolation are of analytical grade. The purities of all compounds were confirmed to be \geq 95% by HPLC/MS analysis (see Supporting Information for details).

Plant Material. Dried flowers of *C. japonica* were purchased from Gangwon Herbs, Kangwon-do, Republic of Korea, on May 2013. The sample was botanically identified by Prof. W. K. Oh, and a voucher specimen (SNU-2013-0012) was deposited at the College of Pharmacy, Seoul National University, Korea.

Extraction and Isolation. The dried *C. japonica* flowers (3.0 kg) was extracted with 70% EtOH (3×15 L, each time for 2 days) at room temperature, which gave a black residue (490 g) after drying. Part of this extract (400 g) was suspended in H₂O (4.0 L) and partitioning against *n*-hexane and *n*-BuOH. The *n*-BuOH portion was selected for further fractionation due to a screening indicating the anti-PEDV activity in *n*-BuOH portion, as analyzed in a CPE assay, which also guided further separation and purification. The *n*-BuOH part (100.2 g) was first subjected to a silica gel CC (15 cm × 60 cm) eluting with a solvent system of *n*-hexane/EtOAc/*n*-BuOH (from 10:1:0.1 to 0:0:1) to give 20 subfractions (CJ1–CJ20). Fraction CJ12 (10.3 g) was further separated by a RP-C₁₈ column (2.0 cm × 30 cm) eluted with MeOH:H₂O (from 1:3 to 5:1) to give 12 subfractions (CJ12.1–CJ12.12). Fraction CJ12.10 (506 mg) was purified on a Gilson HPLC system [mobile phase, MeOH in H₂O containing 0.1% HCO₂H (0–10 min, 75%; 11–40 min, 85%); flow rate, 2 mL/min; UV detection at 205 and 254 nm] giving compounds 3 (6.5 mg; *t*_R = 15.1 min; 2.65×10^{-6} % dry weight of *C. japonica* flowers) and 12 (5.1 mg; *t*_R = 22.2 min; 2.08×10^{-6} % dry weight). Fraction CJ13 (16.0 g) was chromatographed over a RP-C₁₈ column (2.0 cm × 50 cm), eluting with MeOH:H₂O (from 1:10 to 1:0), to yield 15 subfractions (CJ13.1–CJ13.15). Subfraction CJ13.8 (1.1 g) was further separated by Sephadex LH-20 eluting with EtOH to give compound 8 (26.1 mg; 1.07×10^{-5} % dry weight), 9 (200.6 mg; 8.19×10^{-5} % dry weight), and an impurity fraction (661.2 mg), which was purified by HPLC [mobile phase, MeOH in H₂O containing 0.1% HCO₂H (0–20 min, 75%; 21–35 min, 83%); flow rate, 2 mL/min; UV detection at 205 and 254 nm], yielding compounds 6 (10.5 mg; *t*_R = 34.1 min; 4.29×10^{-6} % dry weight), 10 (4.8 mg; *t*_R = 29.5 min; 1.96×10^{-6} % dry weight), 11 (9.6 mg; *t*_R = 32.2 min; 3.92×10^{-6} % dry weight), and 13 (4.6 mg; *t*_R = 28.6 min; 1.88×10^{-6} % dry weight). Fraction CJ13.9 (931.6 mg) was purified by HPLC [mobile phase, MeOH in H₂O containing 0.1% HCO₂H (0–15 min, 60%; 16–45 min, 78%); flow rate, 2 mL/min; UV detection at 205 and 254 nm] to afford compounds 1 (80.3 mg; *t*_R = 32.6 min; 3.28×10^{-5} % dry weight), 2 (50.2 mg; *t*_R = 41.5 min; 2.05×10^{-5} % dry weight), 7 (5.8 mg; *t*_R = 31.2 min; 2.37×10^{-6} % dry weight), and 15 (30.5 mg; *t*_R = 26.1 min; 1.25×10^{-5} % dry weight). Fraction CJ14 (6.1 g) was repeatedly purified by RP-C₁₈ and Sephadex LH-20 CC, eluted mixtures of MeOH and H₂O to give compounds 4 (16.3 mg; 6.66×10^{-6} % dry weight), 5 (9.9 mg; 4.04×10^{-6} % dry weight), and 14 (10.8 mg; 4.41×10^{-6} % dry weight). The purities of compounds 1–15 ($\geq 95\%$) were checked by HPLC/MS with two different UV detection conditions (see Supporting Information for details).

Camellenodiol 3-O-β-D-Glucuronopyranoside (1). White powder; $[\alpha]_D^{25} -50.0$ (c 0.1, MeOH). IR (KBr) ν_{max} 3381, 2891, 1706, 1664, 1456, 1024, 617 cm⁻¹. ¹H NMR (methanol-*d*₄, 500 MHz): δ_H 5.39 (1H, br t, *J* = 3.6 Hz, H-12), 4.37 (1H, d, *J* = 7.7 Hz, H-1'), 3.76 (1H, d, *J* = 8.9 Hz, H-5'), 3.50 (1H, t, *J* = 8.9 Hz, H-4'), 3.36 (1H, t, *J* = 8.9 Hz, H-3'), 3.30 (1H, d, *J* = 11.6 Hz, H-15a), 3.24 (1H, dd, *J* = 8.9, 7.7 Hz, H-2'), 3.17 (1H, dd, *J* = 11.6, 4.0 Hz, H-3), 2.78 (1H, dd, *J* = 11.3, 3.8 Hz, H-18), 2.03 (1H, m, H-22a), 1.73 (1H, overlap, H-9), 1.64 (1H, d, *J* = 11.6 Hz, H-15b), 1.42 (1H, m, H-22b), 1.14, 1.10, 1.06, 0.99, 0.96, 0.86, 0.85 (each 3H, all s, H₃-27, 26, 23, 25, 30, 24, 29), 0.80 (1H, br d, *J* = 11.0 Hz, H-5). ¹³C NMR (methanol-*d*₄, 125 MHz), Table 1. HRFABMS *m/z* 641.3648 [M + Na]⁺ (calcd for C₃₃H₅₄O₉Na, 641.3666).

Camellenodiol 3-O-6'-Methoxy-β-D-glucuronopyranoside (2). White powder; $[\alpha]_D^{25} -31.7$ (c 0.1, MeOH). IR (KBr) ν_{max} 3408, 2911, 1712, 1672, 1497, 1035, 605 cm⁻¹. ¹H NMR (methanol-*d*₄, 500 MHz): δ_H 5.39 (1H, br t, *J* = 3.4 Hz, H-12), 4.37 (1H, d, *J* = 7.7 Hz, H-1'), 3.81 (1H, d, *J* = 9.6 Hz, H-5'), 3.76 (3H, s, OMe), 3.50 (1H, dd, *J* = 9.6, 9.2 Hz, H-4'), 3.35 (1H, t, *J* = 9.2 Hz, H-3'), 3.22 (1H, dd, *J* = 9.2, 7.7 Hz, H-2'), 3.29 (1H, d, *J* = 12.8 Hz, H-15a), 3.15 (1H, dd, *J* = 12.5, 4.6 Hz, H-3), 2.78 (1H, dd, *J* = 10.8, 4.0 Hz, H-18), 2.01 (1H,

m, H-22a), 1.79 (1H, overlap, H-9), 1.63 (1H, d, *J* = 12.8 Hz, H-15b), 1.40 (1H, m, H-22b), 1.14, 1.10, 1.05, 0.98, 0.96, 0.85, 0.85 (each 3H, all s, H₃-27, 26, 23, 25, 30, 24, 29), 0.80 (1H, br d, *J* = 10.3 Hz, H-5). ¹³C NMR (methanol-*d*₄, 125 MHz), Table 1. HRFABMS *m/z* 655.3820 [M + Na]⁺ (calcd for C₃₆H₅₆O₉Na, 655.3822).

Camellenodiol 3-O-6'-Ethoxy-β-D-glucuronopyranoside (3). White powder; $[\alpha]_D^{25} -24.1$ (c 0.1, MeOH). IR (KBr) ν_{max} 3410, 2928, 1712, 1652, 1480, 1015, 621 cm⁻¹. ¹H NMR (methanol-*d*₄, 500 MHz): δ_H 5.39 (1H, br t, *J* = 3.1 Hz, H-12), 4.37 (1H, d, *J* = 7.8 Hz, H-1'), 4.21 (2H, q, *J* = 6.8 Hz, OEt), 3.79 (1H, d, *J* = 9.6 Hz, H-5'), 3.51 (1H, dd, *J* = 9.6, 9.3 Hz, H-4'), 3.35 (1H, t, *J* = 9.3 Hz, H-3'), 3.31 (1H, d, *J* = 12.0 Hz, H-15a), 3.22 (1H, dd, *J* = 9.3, 7.8 Hz, H-2'), 3.16 (1H, dd, *J* = 12.0, 4.1 Hz, H-3), 2.78 (1H, dd, *J* = 11.8, 3.6 Hz, H-18), 2.01 (1H, m, H-22a), 1.76 (1H, overlap, H-9), 1.61 (1H, d, *J* = 12.0 Hz, H-15b), 1.40 (1H, m, H-22b), 1.28 (3H, t, *J* = 6.8 Hz, OEt), 1.14, 1.10, 1.05, 0.98, 0.96, 0.86, 0.86 (each 3H, all s, H₃-27, 26, 23, 25, 30, 24, 29), 0.80 (1H, br d, *J* = 11.2 Hz, H-5). ¹³C NMR (methanol-*d*₄, 125 MHz), Table 1. HRESIMS *m/z* 669.3990 [M + Na]⁺ (calcd for C₃₇H₅₈O₉Na, 669.3979).

Camellenodiol 3-O-[β-D-Glucopyranosyl(1→2)-β-D-galactopyranosyl(1→3)]-β-D-glucuronopyranoside (4). White powder; $[\alpha]_D^{25} -27.0$ (c 0.1, MeOH). IR (KBr) ν_{max} 3411, 2902, 1708, 1661, 1461, 1010, 625 cm⁻¹. ¹H NMR (pyridine-*d*₅, 500 MHz): δ_H 5.46 (1H, br s, H-12), 5.09 (1H, d, *J* = 7.6 Hz, H-1''), 5.06 (1H, d, *J* = 7.6 Hz, H-1'''), 5.01 (1H, d, *J* = 7.8 Hz, H-1'), 4.63 (1H, d, *J* = 8.9 Hz, H-5'), 3.72 (1H, d, *J* = 12.8 Hz, H-15a), 3.32 (1H, dd, *J* = 11.2, 4.0 Hz, H-3), 3.12 (1H, br d, *J* = 11.6 Hz, H-18), 2.52 (1H, br d, *J* = 9.8 Hz, H-22a), 1.96 (1H, d, *J* = 12.8 Hz, H-15b), 1.91 (1H, m, H-22b), 1.54 (1H, t, *J* = 8.1 Hz, H-9), 1.37, 1.29, 1.26, 1.12, 0.92, 0.84, 0.80 (each 3H, all s, H₃-27, 23, 26, 24, 30, 29, 25), 0.75 (1H, br d, *J* = 11.6 Hz, H-5). ¹³C NMR (pyridine-*d*₅, 125 MHz), Table 2. HRFABMS *m/z* 965.4744 [M + Na]⁺ (calcd for C₄₇H₇₄O₁₉Na, 965.4722).

3β-Hydroxy-olean-12,17-dien-16-one 3-O-6'-Methoxy-β-D-glucuronopyranoside (10). White powder; $[\alpha]_D^{25} -20.7$ (c 0.1, MeOH). UV (MeOH) λ_{max} (log ϵ) 298 (4.02) nm. IR (KBr) ν_{max} 3401, 2935, 1731, 1653, 1410, 1136, 612 cm⁻¹. ¹H NMR (CDCl₃, 400 MHz): δ_H 6.12 (1H, br s, H-12), 4.39 (1H, d, *J* = 7.6 Hz, H-1'), 3.86 (1H, d, *J* = 9.6 Hz, H-5'), 3.81 (1H, s, OMe), 3.77 (1H, dd, *J* = 9.6, 8.8 Hz, H-4'), 3.61 (1H, t, *J* = 8.8 Hz, H-3'), 3.50 (1H, dd, *J* = 8.8, 7.6 Hz, H-2'), 3.18 (1H, dd, *J* = 11.5, 4.3 Hz, H-3), 2.60 (1H, d, *J* = 15.1 Hz, H-15a), 2.45 (1H, m, H-22a), 2.14 (1H, d, *J* = 15.1 Hz, H-15b), 2.01 (1H, m, H-22b), 1.56 (1H, m, H-9), 1.10, 1.01, 0.98, 0.94, 0.94, 0.92, 0.85 (each 3H, all s, H₃-27, 23, 25, 30, 26, 29, 24), 0.79 (1H, br d, *J* = 11.6 Hz, H-5). ¹³C NMR (CDCl₃, 100 MHz), Table 1. HRFABMS *m/z* 615.3899 [M + H]⁺ (calcd for C₃₆H₅₆O₈, 615.3897).

3β-Hydroxy-28-norolean-12,17-dien-16-one 3-O-6'-Methoxy-α-D-glucuronopyranoside (11). White powder; $[\alpha]_D^{25} -15.7$ (c 0.1, MeOH). UV (MeOH) λ_{max} (log ϵ) 296 (4.03) nm. IR (KBr) ν_{max} 3434, 2921, 1739, 1658, 1454, 1032, 616 cm⁻¹. ¹H NMR (CDCl₃, 500 MHz): δ_H 6.10 (1H, br s, H-12), 5.13 (1H, d, *J* = 4.0 Hz, H-1'), 4.29 (1H, d, *J* = 9.1 Hz, H-5'), 3.82 (1H, s, OMe), 3.78–3.72 (2H, overlap, H-3' and H-4'), 3.58 (1H, br d, *J* = 8.9 Hz, H-2'), 3.34 (1H, dd, *J* = 11.8, 4.3 Hz, H-3), 2.60 (1H, d, *J* = 15.5 Hz, H-15a), 2.43 (1H, m, H-22a), 2.14 (1H, d, *J* = 15.5 Hz, H-15b), 2.02 (1H, m, H-22b), 1.57 (1H, m, H-9), 1.09, 1.04, 0.98, 0.94, 0.93, 0.90, 0.84 (each 3H, all s, H₃-27, 23, 25, 30, 26, 29, 24), 0.81 (1H, br d, *J* = 10.2 Hz, H-5). ¹³C NMR (CDCl₃, 125 MHz), Table 1. HRFABMS *m/z* 615.3884 [M + H]⁺ (calcd for C₃₆H₅₆O₈, 615.3897).

1β-Hydroxy-olean-12,17-dien-3,12,16-trione (12). White powder; $[\alpha]_D^{25} -10.0$ (c 0.1, MeOH). UV (MeOH) λ_{max} 311 (4.10) nm. IR (KBr) ν_{max} 3420, 2910, 1702, 1645, 1643, 1142, 606 cm⁻¹. ¹H NMR (CDCl₃, 500 MHz): δ_H 6.19 (1H, s, H-12), 5.68 (1H, br s, OH-1), 3.90 (1H, dd, *J* = 8.0, 2.8 Hz, H-1), 2.91 (1H, dd, *J* = 14.2, 7.9 Hz, H-2a), 2.68 (1H, d, *J* = 15.6 Hz, H-15a), 2.66 (1H, s, H-9), 2.56 (1H, m, H-22a), 2.38 (1H, dd, *J* = 14.2, 2.8 Hz, H-2b), 2.37 (1H, d, *J* = 15.6 Hz, H-15b), 2.33 (1H, m, H-22b), 1.34, 1.13, 1.09, 1.07, 0.96, 0.94 (each 3H, all s, H₃-27, 23, 25, 24, 30, 29), 1.43 (1H, overlap, H-5). ¹³C NMR (CDCl₃, 100 MHz), Table 1. HRFABMS *m/z* 453.3035 [M + H]⁺ (calcd for C₂₉H₄₁O₄, 453.3005).

3 β ,16 α -Dihydroxy-olean-12-en-28-ol 3-O- β -D-glucuronopyranoside (13). White powder; $[\alpha]_{D}^{25} -46.4$ (*c* 0.1, MeOH); IR (KBr) ν_{max} 3410, 2910, 1702, 1657, 1441, 1001, 685 cm^{-1} . 1H NMR (methanol-*d*₄, 600 MHz): δ_H 9.21 (1H, s, H-28), 5.40 (1H, br t, *J* = 3.5 Hz, H-12), 4.36 (1H, d, *J* = 7.8 Hz, H-1'), 4.27 (1H, br s, H-16), 3.18 (1H, dd, *J* = 10.6, 3.9 Hz, H-3), 2.66 (1H, dd, *J* = 10.8, 2.3 Hz, H-18), 1.91 (1H, m, H-22a), 1.66 (1H, m, H-22b), 1.63 (1H, t, *J* = 8.7 Hz, H-9), 1.52 (1H, m, H-15a), 1.38, 1.05, 0.96, 0.95, 0.91, 0.85, 0.73 (each 3H, all s, H-27, 23, 30, 25, 29, 24, 26), 1.26 (1H, m, H-15b), 0.77 (1H, br d, *J* = 11.5 Hz, H-5). ^{13}C NMR (methanol-*d*₄, 150 MHz), Table 1. HRESIMS *m/z* 655.3810 [M + Na]⁺ (calcd for C₃₆H₅₆O₉Na, 655.3822).

Echinocystic Acid 3-O-[β -D-Galactopyranosyl(1 \rightarrow 2)]- [β -D-glucopyranosyl(1 \rightarrow 2)- β -D-galactopyranosyl(1 \rightarrow 3)]- β -D-glucuronopyranoside (14). White powder; $[\alpha]_{D}^{25} -18.3$ (*c* 0.1, MeOH). IR (KBr) ν_{max} 3401, 2901, 1711, 1642, 1438, 1023, 1010, 612 cm^{-1} . 1H NMR (methanol-*d*₄, 600 MHz): δ_H 5.25 (1H, br t, *J* = 2.4 Hz, H-12), 5.10 (1H, d, *J* = 7.8 Hz, H-1'''), 4.99 (1H, d, *J* = 7.8 Hz, H-1''), 4.66 (1H, d, *J* = 7.8 Hz, H-1'''), 4.45 (1H, d, *J* = 7.8 Hz, H-1'), 3.79 (1H, br s, H-16), 3.19 (1H, dd, *J* = 11.0, 3.6 Hz, H-3), 2.19 (1H, br d, *J* = 10.0 Hz, H-18), 2.02 (1H, m, H-22a), 1.93 (1H, m, H-15a), 1.62 (1H, m, H-9), 1.57 (1H, m, H-22b), 1.34, 1.09, 1.02, 0.97, 0.94, 0.89, 0.88 (each 3H, all s, H-27, 23, 30, 25, 26, 24, 29), 1.21 (1H, m, H-15b), 0.78 (1H, br d, *J* = 12.0 Hz, H-5). ^{13}C NMR (methanol-*d*₄, 150 MHz), Table 2. HRFABMS *m/z* 1157.5317 [M + Na]⁺ (calcd for C₅₄H₈₀O₂₅Na, 1157.5356).

Determination of the Absolute Configuration of Sugar Components. Each glycoside (2 mg) was hydrolyzed with 1 M HCl (H₂O/ethylene oxide, 1:1, 2 mL) under reflux at 100 °C for 2 h. After dried in vacuo, the residue was subjected to partitioning between H₂O and EtOAc. The H₂O layer was concentrated to give a monosaccharide residue. This residue was dissolved in pyridine (1 mL), and 2 mg of L-cysteine methyl ester hydrochloride was added. This solution was kept at 60 °C for 2 h, and then trimethylsilylimidazole (0.2 mL) was added. The mixture was maintained at 60 °C for another 2 h. After drying the solution, the residue was partitioned between H₂O (2 mL) and *n*-hexane (2 mL). The *n*-hexane layer was analyzed by GC (column, DB-5MS, 30 m × 0.32 mm × 0.25 μ m; detector, FID; detector temperature, 280 °C; injected temperature, 250 °C; column temperature, from 100 to 280 °C with 10 °C/min, then to 300 °C with 20 °C/min, held for 15 min; carrier gas, He). The sugar derivatives showed retention time of 10.37, 13.29, and 19.35 min, identical to the trimethylsilyl-L-cysteine derivatives of authentic D-galactose, D-glucose, and D-glucuronic acid, respectively.

Cell Culture and Virus Stock. Vero cells (African green monkey kidney cell line; ATCC CCR-81) were provided by American Type Culture Collection (ATCC, Manassas, VA, USA) and maintained in Dulbecco's Modified Eagle's Medium (DMEM) with 100 U/mL penicillin, 100 μ g/mL streptomycin, and 10% fetal bovine serum (FBS). PEDV was obtained from Choong Ang Vaccine Laboratory, Korea. Virus stock was kept at -80 °C before use.

Cytotoxicity Assay. The cell viability was calculated using a MTT (3-(4,5-dimethyl-2-thiazolyl)-2,5-diphenyl-2*H*-tetrazolium bromide) assay. Vero cells were grown in 96-well plates at 1 \times 10⁵ cells per well and adhered for 24 h before treatment. The cells were treated with different concentrations of compounds and incubated for 48 h. To avoid solvent toxicity, the final concentration of DMSO was maintained at 0.05% (v/v) in the culture medium. Then, 20 μ L of the 2 mg/mL MTT solution was added to each well and incubated for 4 h. After removing supernatant, 100 μ L of DMSO was added to solubilize formazan crystals. Consequently, the absorbance was measured at 550 nm. Percentage cell viability is determined as the absorbance in the experiment well compared to that in the control wells, and toxicities of the compounds were defined as the percentage cell viability. Regression analysis was used to calculate the 50% cytotoxic concentration (CC₅₀).

Cytopathic Effect (CPE) Inhibition Assay. Vero cells were seeded onto 96-well plates at 1 \times 10⁵ cells per well. One day later, medium was removed and then washed with phosphate buffered saline (PBS). PEDV at 0.01 MOI was inoculated onto near confluent Vero

cell monolayers for 2 h. The media was replaced by DMEM with several compounds at different concentrations. After incubation of 72 h at 37 °C under 5% CO₂ atmosphere, cells were replaced with DMEM and 20 μ L of 2 mg/mL MTT to each well and incubated for 4 h at 37 °C. The 50% effective concentration (EC₅₀) was calculated using regression analysis, and the formula SI = CC₅₀/EC₅₀ was applied to determine the selective index (SI).

Quantitative Real-Time PCR. Vero cells were grown to about 90% confluence in 6-well plates, infected with PEDV at 0.01 MOI, and incubated for 2 h. Then media was replaced by DMEM and cultured with compounds of interest at various concentrations. After 24 h, total RNA was isolated from the cells by following TRIzol method and reverse transcribed using random primer (iNtRON Biotechnology, Inc., Seongnam, Korea) based on manufacturer's instruction. Real-time PCR was performed using selective primers for PEDV, which is listed in Table 2 (Supporting Information) and conducted using 2 μ L of cDNA and Maxima SYBR Green qPCR master mix 2X (Thermo Scientific, Rockford, IL, USA). Cycling conditions for real-time PCR were follows: 95 °C for 10 min, followed by 40 cycles of 95 °C for 15 s, and 60 °C for 1 min. Real-time PCR was conducted using the StepOnePlus Real-Time PCR System (Applied Biosystems, Inc., Foster City, CA, USA). The data was analyzed with StepOne software v2.3.

Western Blot Analysis. The cultures were prepared using similar methods to quantitative real-time PCR. After 24 h, the cells were washed with cold PBS and kept at -80 °C. For whole cell lysate, the cells were lysed on ice in 100 μ L of lysis buffer [50 mM NaF, 0.5% NP-40, 1 mM EDTA, 120 mM NaCl, 50 mM Tris-HCl (pH 7.6)] and centrifuged at 12000 rpm for 20 min. Protein concentrations were calculated using protein assay kit (Bio-Rad Laboratories, Inc., Hercules, CA, USA). After boiling for 5 min, aliquots of lysates were electrophoresed on 10% or 12% SDS-polyacrylamide gels. Protein in the gels were electrotransferred to PVDF membranes (PVDF 0.45 μ m, Immobilon-P, USA). Membranes were incubated with primary antibodies spike (S) protein, nucleocapsid (N) (AbFrontier Co., Ltd., Seoul, Korea), or mouse monoclonal actin antibody and further incubated with secondary antibodies. Finally, they were detected using enhanced chemiluminescence Western blotting detection kit (Thermo Scientific, Rockford, IL, USA).

Immunofluorescence Assay. Vero cells were grown on 8-well chamber slides (LAB-TEK, NUNC, Thermo Fisher Scientific, Waltham, MA, USA) and PEDV at 0.01 MOI were injected to the cell monolayers for 2 h. Then, the solution was replaced by DMEM and treated with compounds of interest. After incubation at 37 °C under 5% CO₂ atmosphere for 24 h, cells were washed with PBS (pH 7.4) three times and fixed with a 4% paraformaldehyde solution for 30 min at room temperature. After blocking with 1% BSA for 1 h, the cells were incubated overnight with monoclonal antibody against N protein of PEDV (AbFrontier Co., Ltd., Seoul, Korea) diluted 1:50 in PBS (pH 7.4). Then the cells were incubated with FITC-conjugated goat antimouse IgG antibody (Jackson ImmunoResearch, Inc., West Grove, PA, USA) for 1 h after washing with PBS (pH 7.4). After washing three times with PBS (pH 7.4), the cells were stained with 500 nM DAPI solution for 10 min at room temperature and washed with PBS (pH 8.0) three times. Slides were mounted with mounting reagent for fluorescence (Vectashield, Vector Laboratories Inc., Burlingame, CA, USA) and observed by fluorescence microscopy (Olympus ix70 Fluorescence Microscope, Olympus Corporation, Tokyo, Japan).

Statistical Analysis. The results are expressed as the means \pm SD of three independent experiments. Statistical analysis was conducted on Sigma Plot Statistical Analysis software, and differences between group mean values were determined by one-way analysis of variance followed by a two-tailed Student's *t*-test for unpaired samples, assuming equal variances. Statistical significance was accepted at *p* < 0.05.

■ ASSOCIATED CONTENT

Supporting Information

Purity check of compounds **1–15** by HPLC/MS analysis, characterization data of compounds **6** and **9**, 1D (^1H and ^{13}C) and 2D (HSQC and HMBC) NMR spectra for new compounds **1–4** and **10–14**, a time-course study, the infectivity of PEDV particles assay, and cell protection assay for compound **9**, inhibitory effects of compounds **6**, **9**, **11**, and **13** on PEDV RNA expression by RT-PCR at the same concentration of $0.25 \mu\text{M}$, inhibitory effects of compounds **1**, **4**, **5**, and **9** on PEDV RNA expression encoding GP6 nucleocapsid protein synthesis by RT-PCR analysis, and the table for primers used for real-time PCR. This material is available free of charge via the Internet at <http://pubs.acs.org>.

■ AUTHOR INFORMATION

Corresponding Author

*Phone/Fax: +82-02-880-7872. E-mail: wkoh1@snu.ac.kr.

Author Contributions

[§]These authors contributed equally to this work.

Notes

The authors declare no competing financial interest.

■ ACKNOWLEDGMENTS

This work was supported in part by grants from the National Research Foundation of Korea (NRF) (NRF-2012R1A2A2A01009417) and from the Procurement and Development of Foreign Biological Resources (2012-K1A1A3307871) funded by the Korean government.

■ ABBREVIATIONS USED

PEDV, porcine epidemic diarrhea virus; GP, glycoprotein; RT-PCR, real time-PCR; CoVs, coronaviruses; N, nucleocapsid; M, membrane; S, spike; E, envelope; SARS, severe acute respiratory syndrome; CCV, canine coronavirus; IBV, infectious bronchitis virus; TGEV, transmissible gastroenteritis coronavirus; EtOH, ethanol; RP-C₁₈, reverse phase-C₁₈; MeOH, methanol; H₂SO₄, sulfuric acid; CPE, cytopathic effect; SI, selective index; CC₅₀, 50% cytotoxic concentration; CC, column chromatography; *n*-BuOH, *n*-butanol; EtOAc, ethyl acetate; HCO₂H, formic acid; KBr, potassium bromide; CDCl₃, deuterated chloroform; HCl, hydrochloric acid; He, helium; ATCC, American Type Culture Collection; DMEM, Dulbecco's Modified Eagle's Medium; FBS, fetal bovine serum; MTT, 3-(4,5-dimethyl-2-thiazolyl)-2,5-diphenyl-2H-tetrazolium bromide; MOI, multiplicity of infection; CO₂, carbon dioxide; qPCR, quantitative PCR; NaF, sodium fluoride; NP-40, Nonidet P-40; NaCl, sodium chloride; PVDF, polyvinylidene difluoride; FITC, fluorescein isothiocyanate; DAPI, 4',6-diamidino-2-phenylindole; SD, standard deviation

■ REFERENCES

- (1) Xing, Y.; Chen, J.; Tu, J.; Zhang, B.; Chen, X.; Shi, H.; Baker, S. C.; Feng, L.; Chen, Z. The papain-like protease of porcine epidemic diarrhea virus negatively regulates type I interferon pathway by acting as a viral deubiquitinase. *J. Gen. Virol.* **2013**, *94*, 1554–1567.
- (2) Park, S. J.; Song, D.-S.; Park, B.-K. Molecular epidemiology and phylogenetic analysis of porcine epidemic diarrhea virus (PEDV) field isolates in Korea. *Arch. Virol.* **2013**, *158*, 1533–1541.
- (3) (a) Li, F. Receptor recognition and cross-species infections of SARS coronavirus. *Antiviral Res.* **2013**, *100*, 246–254. (b) Tsai, K.-C.; Chen, S.-Y.; Liang, P.-H.; Lu, I.-L.; Mahindroo, N.; Hsieh, H.-P.; Chao, Y.-S.; Liu, L.; Liu, D.; Lien, W.; Lin, T.-H.; Wu, S.-Y. Discovery of a novel family of SARS-CoV protease inhibitors by virtual screening and 3D-QSAR studies. *J. Med. Chem.* **2006**, *49*, 3485–3495. (c) Odedra, A.; Lush, S.-F.; Liu, R.-S. Dicobaltoctacarbonyl-mediated synthesis of tricyclic 5,6-dihdropyran-2-one derivatives via tandem cycloaddition reaction between *cis*-epoxyalkynes, a tethered olefin, and carbon monoxide. *J. Org. Chem.* **2007**, *72*, 567–573.
- (4) Drexler, J. F.; Corman, V. M.; Drosten, C. Ecology, evolution and classification of bat coronaviruses in the aftermath of SARS. *Antiviral Res.* **2014**, *101*, 45–56.
- (5) Wang, Y.; Li, J.; Sun, M.; Ni, B.; Huan, C.; Huang, L.; Fan, H.; Ren, X.; Mao, X. Triggering unfolded protein response by 2-deoxy-D-glucose inhibits porcine epidemic diarrhea virus propagation. *Antiviral Res.* **2014**, *106*, 33–41.
- (6) Li, C.; Li, Z.; Zou, Y.; Wicht, O.; van Kuppevel, F. J. M.; Rottier, P. J. M.; Bosch, B. J. Manipulation of the porcine epidemic diarrhea virus genome using targeted RNA recombination. *PLoS One* **2013**, *8*, e69997:1–9.
- (7) Mole, B. Deadly pig virus slips through US borders. *Nature* **2013**, *499*, 388.
- (8) Sun, R.-Q.; Cai, R.-J.; Chen, Y.-Q.; Liang, P.-S.; Chen, D.-K.; Song, C.-X. Outbreak of porcine epidemic diarrhea in suckling piglets, China. *Emerg. Infect. Dis.* **2012**, *18*, 161–163.
- (9) Schwartz, K.; Main, R. Porcine epidemic diarrhea (PED) virus: FAQ and survival tips. *National Hog Farmer* **2013**, July, <http://nationalhogfarmer.com/health/porcine-epidemic-diarrhea-ped-virus-faq-and-survival-tips>.
- (10) Peng, H.-K.; Chen, W.-C.; Lin, Y.-T.; Tseng, C.-K.; Yang, S.-Y.; Tzeng, C.-C.; Lee, J.-C.; Yang, S.-C. Anti-hepatitis C virus RdRp activity and replication of novel anilinobenzothiazole derivatives. *Antiviral Res.* **2013**, *100*, 269–275.
- (11) Choi, H.-J.; Kim, J.-H.; Lee, C.-H.; Ahn, Y.-J.; Song, J.-H.; Baek, S.-H.; Kwon, D.-H. Antiviral activity of quercetin 7-rhamnoside against porcine epidemic diarrhea virus. *Antiviral Res.* **2009**, *81*, 77–81.
- (12) Song, D. S.; Oh, J. S.; Kang, B. K.; Yang, J. S.; Moon, H. J.; Yoo, H. S.; Jang, Y. S.; Park, B. K. Oral efficacy of Vero cell attenuated porcine epidemic diarrhea virus DR13 strain. *Res. Vet. Sci.* **2007**, *82*, 134–140.
- (13) (a) Belema, M.; Meanwell, N. A. Discovery of daclatasvir, a pan-genotypic hepatitis C virus NSSA replication complex inhibitor with potent clinical effect. *J. Med. Chem.* **2014**, *57*, 5057–5071. (b) Gigante, A.; Canela, M.-D.; Delang, L.; Priego, E.-M.; Camarasa, M.-J.; Querat, G.; Neyts, J.; Leyssen, P.; Pérez-Pérez, M.-J. Identification of [1,2,3]triazolo[4,5-*d*]pyrimidin-7(6*H*)-ones as novel inhibitors of chikungunya virus replication. *J. Med. Chem.* **2014**, *57*, 4000–4008.
- (d) Li, T.; Peng, T. Traditional Chinese herbal medicine as a source of molecules with antiviral activity. *Antiviral Res.* **2013**, *97*, 1–9.
- (e) Baker, T. J.; Luedtke, N. W.; Tor, Y.; Goodman, M. Synthesis and anti-HIV activity of guanidinoglycosides. *J. Org. Chem.* **2000**, *65*, 9054–9058.
- (14) (a) Scognamiglio, M.; D'Abrosca, B.; Fiumano, V.; Chambery, A.; Severino, V.; Tsafantakis, N.; Pacifico, S.; Esposito, A.; Fiorentino, A. Oleanane saponins from *Bellis sylvestris* Cyr. and evaluation of their phytotoxicity on *Aegilops geniculata* Roth. *Phytochemistry* **2012**, *84*, 125–134. (b) Germonprez, N.; Maes, L.; Puyvelde, L. V.; Tri, M. V.; Tuan, D. A.; Kimpe, N. D. In vitro and in vivo anti-leishmanial activity of triterpenoid saponins isolated from *Maesa balansae* and some chemical derivatives. *J. Med. Chem.* **2005**, *48*, 32–37. (c) Germonprez, N.; Puyvelde, L. V.; Maes, L.; Tri, M. V.; Kimpe, N. D. New pentacyclic triterpene saponins with strong anti-leishmanial activity from the leaves of *Maesa balansae*. *Tetrahedron* **2004**, *60*, 219–228.
- (d) Yu, F.; Wang, Q.; Zhang, Z.; Peng, Y.; Qiu, Y.; Shi, Y.; Zheng, Y.; Xiao, S.; Wang, H.; Huang, X.; Zhu, L.; Chen, K.; Zhao, C.; Zhang, C.; Yu, M.; Sun, D.; Zhang, L.; Zhou, D. Development of oleanane-type triterpenes as a new class of HCV entry inhibitors. *J. Med. Chem.* **2013**, *56*, 4300–4319. (e) Gilabert-Oriol, R.; Mergel, K.; Thakur, M.; von Mallinckrodt, B.; Melzig, M. F.; Fuchs, H.; Weng, A. Real-time analysis of membrane permeabilizing effects of oleanane saponins. *Bioorg. Med. Chem.* **2013**, *21*, 2387–2395. (f) Gauthier, C.; Legault, J.; Girard-Lalancette, K.; Mshvildadze, V.; Pichette, A. Haemolytic activity,

- cytotoxicity and membrane cell permeabilization of semi-synthetic and natural lupane- and oleanane-type saponins. *Bioorg. Med. Chem.* **2009**, *17*, 2002–2008. (g) Baltina, L. A. Chemical modification of glycyrrhetic acid as a route to new bioactive compounds for medicine. *Curr. Med. Chem.* **2003**, *10*, 155–171.
- (15) (a) Tamaru, S.; Ohmachi, K.; Miyata, Y.; Tanaka, T.; Kubayasi, T.; Nagata, Y.; Tanaka, K. Hypotriglyceridemic potential of fermented mixed tea made with third-crop green tea leaves and *Camellia* (*Camellia japonica*) leaves in Sprague–Dawley rats. *J. Agric. Food Chem.* **2013**, *61*, 5817–5823. (b) Nakamura, S.; Fujimoto, S.; Nakashima, S.; Matsumoto, T.; Miura, T.; Uno, K.; Matsuda, H.; Yoshikawa, M. Medicinal flowers. XXXVI. I. Acylated oleanane-type triterpene saponins with inhibitory effects on melanogenesis from the flower buds of Chinese *Camellia japonica*. *Chem. Pharm. Bull.* **2012**, *60*, 752–758.
- (16) (a) Nakamura, S.; Moriura, T.; Park, S.; Fujimoto, K.; Matsumoto, T.; Ohta, T.; Matsuda, H.; Yoshikawa, H. Melanogenesis inhibitory and fibroblast proliferation accelerating effects of noroleanane- and oleanane-type triterpene oligoglycosides from the flower buds of *Camellia japonica*. *J. Nat. Prod.* **2012**, *75*, 1425–1430. (b) Thao, N. T. P.; Hung, T. M.; Lee, M. K.; Kim, J. C.; Min, B. S.; Bae, K. H. Triterpenoids from *Camellia japonica* and their cytotoxic activity. *Chem. Pharm. Bull.* **2010**, *58*, 121–124.
- (17) (a) Ren, Y.; Lantvit, D. D.; Deng, Y.; Kanagasabai, R.; Gallucci, J. C.; Ninh, T. N.; Chai, H.-B.; Soejarto, D. D.; Fuchs, J. R.; Yalowich, J. C.; Yu, J.; Swanson, S. M.; Kinghorn, A. D. Potent cytotoxic arylnaphthalene lignan lactones from *Phyllanthus poilanei*. *J. Nat. Prod.* **2014**, *77*, 1494–1504. (b) Yu, H.-Y.; Chen, Z.-Y.; Sun, B.; Liu, J.; Meng, F.-Y.; Liu, Y.; Tian, T.; Jin, A.; Ruan, H.-L. Lignans from the fruit of *Schisandra glaucescens* with antioxidant and neuroprotective properties. *J. Nat. Prod.* **2014**, *77*, 1311–1320. (c) Lee, K.-T.; Choi, J.; Tung, W.-T.; Nam, J.-H.; Jung, H.-J.; Park, H.-J. Structure of a new echinocystic acid bisdesmoside isolated from *Codonopsis lanceolata* roots and the cytotoxic activity of prosapogenins. *J. Agric. Food Chem.* **2002**, *50*, 4190–4193.
- (18) (a) Beelders, T.; Brand, D. J.; de Beer, D.; Malherbe, C. J.; Mazibuko, S. E.; Muller, C. J. F.; Joubert, E. Benzophenone C- and O-glucosides from *Cyclopia genistoides* (Honeybush) inhibit mammalian α -glucosidase. *J. Nat. Prod.* **2014**, *77*, 2694–2699 DOI: 10.1021/np5007247. (b) Magid, A. A.; Voutquenne, L.; Moretti, C.; Long, C.; Lavaud, C. Triterpenoid saponins from the fruits of *Caryocar glabrum*. *J. Nat. Prod.* **2006**, *69*, 196–205. (c) Cai, W.-H.; Matsunami, K.; Otsuka, H.; Shinzato, T.; Takeda, Y. A glycerol α -D-glucuronide and a megastigmane glycoside from the leaves of *Guettarda speciosa* L. *J. Nat. Med.* **2011**, *65*, 364–369. (d) Shi, S.; Jiang, D.; Dong, C.; Tu, P. Triterpene saponins from *Clematis mandshurica*. *J. Nat. Prod.* **2006**, *69*, 1591–1595. (e) Morikawa, T.; Tao, J.; Toguchida, I.; Matsuda, H.; Yoshikawa, M. Structures of new cyclic diarylheptanoids and inhibitors of nitric oxide production from Japanese folk medicine *Acer nikoense*. *J. Nat. Prod.* **2003**, *66*, 86–91.
- (19) Yoshikawa, M.; Morikawa, T.; Asao, Y.; Fujiwara, E.; Nalamura, S.; Matsuda, H. Medicinal flowers. XV. I. The structures of noroleanane- and oleanane-type triterpene oligoglycosides with gastroprotective and platelet aggregation activities from flower buds of *Camellia japonica*. *Chem. Pharm. Bull.* **2007**, *55*, 606–612.
- (20) Gan, M.; Liu, M.; Gan, L.; Lin, S.; Liu, B.; Zhang, Y.; Zi, J.; Song, W.; Shi, J. Dammarane glycosides from the root of *Machilus yaoshensis*. *J. Nat. Prod.* **2012**, *75*, 1373–1382.
- (21) Puapairoj, P.; Naengchomnong, W.; Kijjoa, A.; Pinto, M. M.; Pedro, M.; Nascimento, M. S. J.; Silva, A. M. S.; Herz, W. Cytotoxic activity of lupane-type triterpenes from *Glochidion sphaerogynum* and *Glochidion eriocarpum* two of which induce apoptosis. *Planta Med.* **2005**, *71*, 208–213.
- (22) Machocho, A. K.; Kiprono, P. C.; Grinberg, S.; Bittner, S. Pentacyclic triterpenoids from *Embelia schimperi*. *Phytochemistry* **2003**, *62*, 573–577.
- (23) (a) Itokawa, H.; Nakajima, H.; Ikuta, A.; Itaka, Y. Two triterpenes from the flowers of *Camellia japonica*. *Phytochemistry* **1981**, *20*, 2539–2542. (b) Nagata, T.; Tsushima, T.; Hamaya, E.; Enoki, N.; Manabe, S.; Nishino, C. Camellidins, antifungal saponins isolated from *Camellia japonica*. *Agric. Biol. Chem.* **1985**, *49*, 1181–1186.
- (24) Calis, I. Saponin and sapogenol. II. The main saponin from the roots and rhizomes of *Primula auriculata*, *P. megaseifolia* and *P. longipes* (Primulaceae). *Turk Saglik Bilimleri Dergisi* **1989**, *13*, 111–120.
- (25) Song, D.; Park, B. Porcine epidemic diarrhoea virus: a comprehensive review of molecular epidemiology, diagnosis, and vaccines. *Virus Genes* **2012**, *44*, 167–175.
- (26) Cruz, D. J.; Kim, C. J.; Shin, H. J. The GPRLQPY motif located at the carboxy-terminal of the spike protein induces antibodies that neutralize porcine epidemic diarrhea virus. *Virus Res.* **2008**, *132*, 192–196.
- (27) Nguyen, V. P.; Hogue, B. G. Protein interactions during Coronavirus assembly. *J. Virol.* **1997**, *71*, 9278–9284.
- (28) Curtis, K. M.; Yount, B.; Baric, R. S. Heterologous gene expression from transmissible gastroenteritis virus replicon particles. *J. Virol.* **2002**, *76*, 1422–1434.
- (29) Park, J. C.; Hur, J. M.; Park, J. G.; Hatano, T.; Yoshida, T.; Miyashiro, H.; Min, B. S.; Hattori, M. Inhibitory effects of Korean medicinal plants and camelliatannin H from *Camellia japonica* on human immunodeficiency virus type 1 protease. *Phytother. Res.* **2002**, *16*, 422–426.
- (30) Enjuanes, L.; DeDiego, M. L.; Alvarez, E.; Deming, D.; Sheahan, T.; Baric, R. Vaccines to prevent severe acute respiratory syndrome coronavirus-induced disease. *Virus Res.* **2008**, *133*, 45–62.